Understanding the Cause of a Long-term Increase in Red Tide Frequency in Nueces-Corpus Christi Bay

Final Report

CMP project #20-042
March 2022

Prepared by:

Michael S. Wetz, Principal Investigator; Sarah Tominack, Ph.D. student
Texas A&M University-Corpus Christi
6300 Ocean Dr., Unit 5869
Corpus Christi, Texas 78412
Phone: 361-825-2132
Email: michael.wetz@tamucc.edu

Submitted to:
Texas General Land Office
1700 Congress Ave.
Austin, TX 78701-1495

A report funded by a Texas Coastal Management Program Grant approved by the Texas Land Commissioner pursuant to National Oceanic and Atmospheric Administration Award No. NA19NOS4190106.

Table of Contents

Executive Summary

Karenia brevis is an unarmored, toxin producing dinoflagellate that is known to is harmful to both human health and that of marine life. Blooms typically start in offshore waters and are advected into nearshore or estuarine waters by currents. While there is a considerable body of knowledge on the ecology of this organism, less is known about factors affecting bloom potential in estuaries where sharp salinity and nutrient gradients may exist that create conditions much more complicated than in offshore waters. To better understand factors leading to the success (or failure) of *K. brevis* red tides in Corpus Christi Bay, we took a three-fold approach: 1) field sampling to quantify phytoplankton (incl. *K. brevis*) dynamics and environmental drivers in the Corpus Christi Bay system over a 27-month period , 2) application of multivariate statistical techniques to determine environmental factors related to *K. brevis* presence-absence, and 3) growth experiments to quantify the influence of salinity and different nutrient sources on *K. brevis* growth. In Corpus Christi Bay, environmental conditions that tend to favor diatoms (i.e., high freshwater inflow, decreased salinity, increased nutrients, cooler temperatures) were found to discourage the formation of a high biomass red tide despite the presence of *K. brevis*. The relationship with salinity, however, was found to be more nuanced than previously thought. Salinity within the Corpus Christi Bay system was found to exceed the optimum range of *K. brevis* more frequently (> 35; 20% of the time) than it was found to be below the salinity barrier proposed in the literature (< 24; ~8% of the time). This indicates that to predict and manage the occurrence of *K. brevis* red tides it will be critical to better understand the role salinity and discharge play in supporting or discouraging red tide formation. Likewise, results from the growth experiments show a strong influence of salinity. Overall, highest growth rates were observed at a salinity of 25, while growth rates were much lower at salinity of 35, and we were

not able to grow the organism at salinities of 15 and 45. Results from the experiment conducted at a salinity of 25 showed that *K. brevis* was able to grow on any of the diverse array of nitrogen sources, including simple compounds of ammonium and nitrate as well as more complex sources from porewater, wastewater and dead fish. In the context of bloom dynamics and influences in local estuaries (to Nueces and Corpus Christi Bays), these findings indicate that it would be difficult to identify and manage specific nutrient sources to reduce bloom potential, especially when considering the multitude of possible internal and external sources to those bays.

Background

Karenia brevis is an unarmored, toxin producing dinoflagellate endemic to the Gulf of Mexico (GoM). It was discovered as the causative agent of Florida (FL) and Texas (TX) red tides in the late 1940s (Davis 1948; Brand et al. 2012). Discolored water accompanied by dead fish and noxious fumes, characteristic of *K. brevis* red tides, have been documented to occur along US GoM coastlines as early as 1844, though these historical occurrences were not as frequent as they are today (Magaña et al. 2003; Brand and Compton 2007). In the US, *K. brevis* red tides are most common along the FL and TX GoM coastlines, though blooms have been transported to the FL Atlantic coast and as far as the North Carolina coast (Brand et al. 2012; Hart et al. 2015; Harris et al. 2020). *K. brevis* red tides typically begin during late summer-early fall, can be short or long-lived (~ 18 months), and can be patchy or extend over many kilometers. Blooms have been shown to cause widespread disruptions to local ecosystems and economies (Baden and Mende 1979; Tester and Steidinger 1997; Vargo 2009; Brand et al. 2012; Tominack et al. 2020).

Symptoms of red tides can include, but are not limited to, fish kills, shellfisheries closures, hypoxic bottom waters, loss of benthic community biomass and diversity (seagrasses and invertebrates), marine mammal and seabird mortality, and respiratory and digestive distress in humans (Aldrich and Wilson 1960; Magaña and Villareal 2006; Maier Brown et al. 2006; Brand et al. 2012). In both FL and TX there is evidence that *K. brevis* red tides can be transported into estuaries where human population centers are in closer proximity (Buskey 1996; Flaherty and Landsberg 2011; McHugh et al. 2011; Walters et al. 2013; Hart et al. 2015; Harris et al. 2020), though there has been limited work regarding *K. brevis* ecology in the estuarine

environment (Steidinger and Ingle 1972; Landsberg and Steidinger 1988; Steidinger 2009). Given evidence of increases in the frequency of red tides and the intrusion of bloom biomass into estuarine environments (Flaherty and Landsberg 2011; McHugh et al. 2011; Walters et al. 2013; Hart et al. 2015; Harris et al. 2020; Tominack et al. 2020) it is important to quantify environmental and climatological variability associated with the success and failure of *K. brevis* red tides in the estuarine environment. An additional concern in TX is the recent introduction of commercial oyster aquaculture in estuaries as allowed by House Bill 1300. Though oysters and are not thought to be directly harmed by *K. brevis* red tides, brevetoxin can accumulate in their tissues causing gastrointestinal distress in humans when consumed (Steidinger 2009; Brand et al. 2012). A more in depth understanding of red tides will therefore be important in predicting conditions that could stand in the way of successful harvest (closures due to red tides) or harm reef associated communities (deoxygenation of bottom waters).

K. brevis red tides consist of three stages; initiation, maintenance, and decline. Maximum growth rates of *K. brevis* are relatively slow (0.2 – 0.5 day^{-1}) compared other phytoplankton taxa (i.e., diatoms), indicating that factors limiting growth rates (i.e., nutrients, light, grazing) are likely less important in driving biomass accumulation during the initiation phase of bloom development (Magaña and Villareal 2006; Paerl and Justić 2013). Current research indicates that the initiation phase is strongly driven by physical mechanisms that act to concentrate biomass in the offshore environment and subsequently transport it shoreward, though the precise pathways for each GoM region vary (Tester and Steidinger 1997; Hetland and Campbell 2007). For TX red tides the current understanding of the transport pathway is as follows: 1) transport of seed populations of *K. brevis* from southern GoM (Bay of Campeche region) to north-northwestern GoM, 2) transition to downcoast winds from summer into fall, where 3) either strong downcoast

winds transport *K. brevis* biomass away from the TX coastline, or weak downcoast winds induce coastward Ekman transport of *K. brevis* biomass to the nearshore environment (Stumpf et al. 2008; Thyng et al. 2013; Henrichs et al. 2015; Henrichs et al. 2018).

General knowledge of *K. brevis* physiology and ecology provides a picture of conditions that are likely necessary for prolonged support of high biomass red tides. *K. brevis* is mixotrophic, capable of utilizing dissolved organic and inorganic compounds as well as phagotrophy of smaller celled organisms (i.e., *Synechococcus* spp.) (Jeong et al. 2005; Glibert et al. 2009; Steidinger 2009; Brand et al. 2012; Dixon et al. 2014; Heil et al. 2014). Previous work in FL waters has demonstrated that *K. brevis* relies on a variety of nutrient sources, based on lack of sufficient N from a single identified source and isotopic evidence of variable nutrient source utilization (Vargo et al. 2008; Walsh et al. 2009). Combined, this indicates that the nutritional flexibility of *K. brevis* is likely a key factor acting to sustain the maintenance phase of red tides and that anthropogenic eutrophication may not be as important for *K. brevis* as for other less nutritionally diverse harmful algal bloom formers (Vargo 2009; Dixon et al. 2014; Heil et al. 2014). *K. brevis* also produces a suite of toxins, some of which are thought to affect the growth of other phytoplankton (Prince et al. 2008; Prince et al. 2010; Poulson-Ellestad et al. 2014) and others of which are thought to affect grazers (i.e., copepods, rotifers) by eliciting prey avoidance or toxic effects on survival, growth, and/or reproduction (Breier and Buskey 2007; Kubanek et al. 2007; Waggett et al. 2012; Walsh and O'Neil 2014). This reduction in competitive stress and grazing potential provides another mechanism by which high biomass red tides can persist for long periods of time. Outside of direct top-down and bottom-up controls on *K. brevis*, salinity and temperature also influence the duration of the maintenance phase of red tides. Findings from field and experimental work indicate that ocean-like salinities (~ 30-35) and fall-like

temperatures (22-28°C) are optimum for *K. brevis* survival and growth (Aldrich and Wilson 1960; Magaña and Villareal 2006; Vargo 2009; Errera et al. 2014). Excessive precipitation or drought conditions therefore have the potential to either halt the transition from initiation phase to maintenance phase (i.e., *K. brevis* is transported to coast but doesn't bloom) as well as affect the duration of the maintenance phase and the extent of bloom dispersion. Early in the literature a barrier for the dispersion of red tides was proposed to be at salinities of ~ 24, and although there have been observations of *K. brevis* in extremely low salinities (~ 5), this barrier has been found to generally hold true (Maier-Brown et al. 2006; Magaña and Villareal 2006; Vargo 2009; Dixon et al. 2014). Seasonal temperature changes are similarly important in supporting the transition from initiation to maintenance phase and the duration of the maintenance phase. Tominack et al. (2020) demonstrated the importance of the transition from summer- to fall-like temperatures at the transition from before bloom to during bloom conditions in the Nueces Estuary.

Mechanisms leading to the decline of *K. brevis* red tides are varied, though few studies have documented the relative importance of each. Abrupt decreases in temperature and strong wind-driven mixing associated with frontal systems have been hypothesized to play a role in bloom decline based on documented preference for relatively warm conditions (22 – 28°C) and lysed cells/aerosolized brevetoxin due to crashing waves (Magaña and Villareal 2006; Vargo 2009). Increased flushing and/or decreased salinity following the passage of winter storms is also a potential contributor to the decline of red tides due to documented preferences for relatively high salinity (~ 30 – 35) and inability to replace washed out biomass (Aldrich and Wilson 1960; Steidinger and Ingle 1972; Magaña and Villareal 2006; Vargo 2009; Errera et al. 2014). Findings from Tominack et al. (2020) provided further support for the role of increased wind speed as

contributing to bloom demise. Lastly, viral lysis and algicidal bacterial activity have also been hypothesized to play a role in bloom decline, though there is limited evidence supporting a strong role for these mechanisms (Doucette et al. 1999; Paul et al. 2002; Roth et al. 2008).

Task 1: Phytoplankton dynamics in Corpus Christi Bay

Introduction

Corpus Christi Bay is located on the South Texas Coast and is bordered by the cities of Corpus Christi, Portland, and Ingleside. The bay is shallow (~ 3 m, ship channel ~ 15 m), microtidal (~ 0.3 m range), and influenced by the relatively high winds (~ 18 km h^{-1} annual mean) characteristic of the region (Ritter and Montagna 1999; Islam et al. 2014; Turner et al. 2015). The regional climate is semi-arid, though increased precipitation and decreased salinity are known to occur associated with El Niño conditions (Tolan 2007). Due to relatively low mean annual precipitation (~ 80 cm yr^{-1}) and very low riverine inflow from the highly altered Nueces River (Montagna et al. 2009), Corpus Christi Bay tends to have long residence times (> 5 mo. – 1 year) and ocean-like salinity, making it conducive to supporting *K. brevis* red tides in close proximity to areas of dense human population. Lastly, Tominack et al. (2020) found that red tides are occurring with increasing frequency within the Corpus Christi Bay system (Nueces Estuary) and that this is potentially related to long term increases in salinity documented throughout the system (Bugica et al. 2020).

To better understand factors leading to the success (or failure) of *K. brevis* red tides in this system, and how climate change may affect this system in the future, this study took a multifaceted approach. We quantified phytoplankton dynamics and environmental drivers in the Corpus Christi Bay system over a 27-month period to provide a more robust understanding of phytoplankton ecology in this estuary and its potential to support red tide blooms. To determine if there were environmental differences in years when *K. brevis* was present and bloomed (discolored water confirmed to be *K. brevis*), present but did not bloom, or was absent, multivariate techniques were used to assess data collected in the late summer-early fall of 2016

through 2020, followed by modeling analyses to determine environmental factors related to *K. brevis* presence-absence (2016-2020) and *K. brevis* abundance (2016-2018). Lastly, variability in phytoplankton community composition and environmental drivers were quantified during the late summer-early fall period of 2016, 2017, and 2018 to further investigate factors related to the success of *K. brevis* during 2016 compared to 2017 and 2018 when *K. brevis* was present but did not reach bloom densities. This study expands what is known about phytoplankton ecology in a low inflow estuary and furthers our understanding of *K. brevis* dynamics in an estuarine environment.

Methods

Sampling Sites

Sampling sites were selected to represent a range of conditions within Corpus Christi Bay (Fig. 1). Four sites were accessed from piers and bridges near the shoreline of Corpus Christi Bay from August 2016 through October 2018 and from February 2020 through October 2020: Packery Channel, Oso Inlet, Cole Park, and South Shore. Packery Channel is a man-man inlet between the Gulf of Mexico and the Upper Laguna Madre/Lower Corpus Christi Bay. Oso Inlet is at the confluence of Oso Bay and Corpus Christi Bay, with freshwater sources including Oso Creek and a nearby WWTP effluent pipe.

Figure 1. Map of sampling locations in Corpus Christi Bay.

Cole Park was located directly in front of a stormwater runoff drain on the western shoreline of Corpus Christi Bay. The South Shore site was located along the southern shoreline of Corpus Christi Bay. Three additional sites were accessed by boat and were sampled from March 2018 through October 2020. The NC confluence site was located near Indian Point, where Nueces and Corpus Christi Bays meet. The Ship Channel site was located near the center of Corpus Christi Bay and the Shamrock Cove site was located in the eastern portion of the bay near Mustang Island. Temporal frequency of sampling was variable based on the project design for the different groups of sites (Table 1).

Table 1. Temporal coverage and resolution captured by sampling at each of the sites used in this analysis.

Site	Date Range Sampled	Sampling Frequency
Packery Channel	8/2016 – 10/2018; 2/2020 – 12/2020	Winter – monthly Spring & Summer – twice monthly Fall – weekly
Oso Inlet	8/2016 – 10/2018; 2/2020 – 12/2020	Winter – monthly Spring & Summer – twice monthly Fall – weekly
Cole Park	8/2016 – 10/2018; 2/2020 – 12/2020	Winter – monthly Spring & Summer – twice monthly Fall – weekly
South Shore	8/2016 – 10/2018; 2/2020 – 12/2020	Winter – monthly Spring & Summer – twice monthly Fall – weekly
Nueces-Corpus Connection	3/2018 – 10/2020	Monthly
Ship Channel	3/2018 – 10/2020	Monthly
Shamrock Cove	3/2018 – 10/2020	Monthly

Field Sampling

Surface water hydrographic data (temperature, conductivity (salinity), pH, dissolved oxygen) were collected using a calibrated YSI ProPlus multiparameter sonde (YSI Inc., Yellow

Springs, Ohio). Water samples were collected from the top 15 cm of the water surface and transported to the lab in acid-washed amber polycarbonate bottles for further processing. Water for micro- and nanophytoplankton enumeration (500 mL) was stored at ambient temperature, while samples for nutrient chemistry, chlorophyll *a* analysis, and picophytoplankton cell counts were stored on ice (~ 0°C) until return to the lab (< 3 hours).

Laboratory Processing

Prior to sample processing, the collection bottles were gently inverted to homogenize the water and suspended materials. Water for micro- and nanophytoplankton enumeration was gently poured into 50 mL conical vials and fixed with acidified Lugol's solution to a final concentration of 1% and stored at room temperature in the dark. Water for dissolved nutrient (ammonium, nitrate plus nitrite, orthophosphate, silicate, dissolved organic carbon and total dissolved nitrogen) quantification was filtered through pre-combusted (4 hours at 450°C) Ahlstrom GF/F filters into HDPE bottles. For picophytoplankton quantification, site water was fixed with 50% glutaraldehyde to a final concentration of 1%. Following sample processing described above, all samples were immediately stored at -20°C until analysis.

Phytoplankton Data

For all sampling dates, live phytoplankton samples were screened and all taxa present were recorded to lowest possible taxonomic classification. Phytoplankton were also enumerated from samples collected from August 2016 through October 2018 at the Packery Channel, Oso Inlet, Cole Park, and South Shore sites. Micro- and nanophytoplankton were counted by following the Utermöhl method on an Olympus IX71 inverted microscope at 200x magnification. The volume settled for each sample was variable based on chlorophyll *a* concentration and the amount of suspended solids noted during live screens. All samples were

settled overnight (> 12 hrs), allowing more than 1 hour of settling time per mL of sample settled. Picophytoplankton were counted using an Accuri C6 Plus flow cytometer with the CSampler Plus adapter (Beckton Dickinson, San Jose, CA). Instrument QC was performed daily following manufacturer protocol prior to sample preparation. Samples were thawed at 0°C in the dark and gently filtered across 20 µm Nytex® mesh to remove large cells and particulate matter. All samples were run on the fast setting, with a flow rate of 66 µL min^{-1} and a core size of 22 µm. The auto-sampler was set to agitate the sampling plate and rinse the sample input port before and after each sample was analyzed. Additionally, polystyrene beads of known size (3.3 µm) were run at the same settings to ensure that only appropriate size ranges of cells were counted. Biovolumes were estimated for micro-, nano-, and picophytoplankton using the associated geometric shapes at the lowest taxonomic resolution recorded during counting (Sun and Liu, 2003). Picophytoplankton shape and size was not directly measured and was estimated to be spherical at 1.5 µm and 2.5 µm diameters for picocyanobacteria and picoeukaryotes, respectively.

Nutrients

Inorganic nutrient samples were thawed to room temperature and then analyzed on a Seal QuAAtro autoanalyzer. Standard curves with five different concentrations were run daily at the beginning of each run. Fresh standards were made prior to each run by diluting a primary standard with low nutrient surface seawater. Deionized water (DIW) was used as a blank, and DIW blanks were run at the beginning and end of each run, as well as after every 8–10 samples to correct for baseline shifts. Method detection limits were 0.02 µM for nitrate plus nitrite (NO_x) and ammonium (NH_4^+), and < 0.01 µM for orthophosphate (PO_4^{3-}) and silicate (SiO_4). Dissolved inorganic nitrogen (DIN) was calculated as the sum of NH_4^+ and NOx. Samples for dissolved

organic carbon (DOC) and total dissolved nitrogen (TDN) were thawed to room temperature and analyzed using the High Temperature Catalytic Oxidation method on a Shimadzu TOC-Vs analyzer with nitrogen module. Standard curves were run twice daily using a DIW blank and five concentrations of either acid potassium phthalate solution or potassium nitrate for DOC and TDN, respectively. Three to five subsamples were taken from each standard and water sample and injected in sequence. Reagent grade glucosamine was used as a laboratory check standard and inserted throughout each run, as were Certified Reference Material Program (CRMP) deep-water standards of known DOC/TDN concentration. Dissolved organic nitrogen (DON) was determined by subtracting dissolved inorganic nitrogen (NH_4^+ and NO_x) from TDN.

Accessory Data Collection

Daily precipitation totals were downloaded from the NOAA National Climate Data Center for five weather stations around Corpus Christi Bay (USC00412013, USW00012946, USW00012926, USC00417176, USC00417170; accessed 11/16/2021). Data from the five weather stations were averaged together by data and rolling 5-day precipitation totals were also calculated from this dataset. Daily discharge data was downloaded from the USGS (https://waterdata.usgs.gov) for the Nueces River at Mathis, TX (USGS 08211000) and Oso Creek at Corpus Christi, TX (USGS 08211520). Riverine discharge into Corpus Christi Bay was calculated as the sum of the mean daily discharge at both gauge sites. Wind speed and direction data were downloaded from the NOAA National Data Buoy Center (https://www.ndbc.noaa.gov/historical_data.shtml) for the Bob Hall Pier Buoy (MQTT2). Daily average wind speed and wind vectors were calculated from six-minute averages of wind speed and direction. The nature of wind direction data is such that a predominantly N wind could be represented by either 358° or 2°, making means of wind direction difficult to interpret. The

calculation of U (east-west wind speed) and V (north-south wind speed) vectors and subsequent averaging more accurately represent the magnitude of winds along east-west and north-south trajectories. U was calculated using the formula $U = \cos\left((270 - wind\ direction) \times \frac{\pi}{180}\right) \times wind\ speed$ and V was calculated using the formula $V = \sin\left((270 - wind\ direction) \times \frac{\pi}{180}\right) \times wind\ speed$. Data were subsequently averaged by date to create a daily wind speed and vector components data set. The number of named storms affecting the western Gulf of Mexico for each study year was determined by using the interactive historical hurricane track map provided by NOAA (https://coast.noaa.gov/hurricanes/#map=4/32/-80) (Fig. 2).

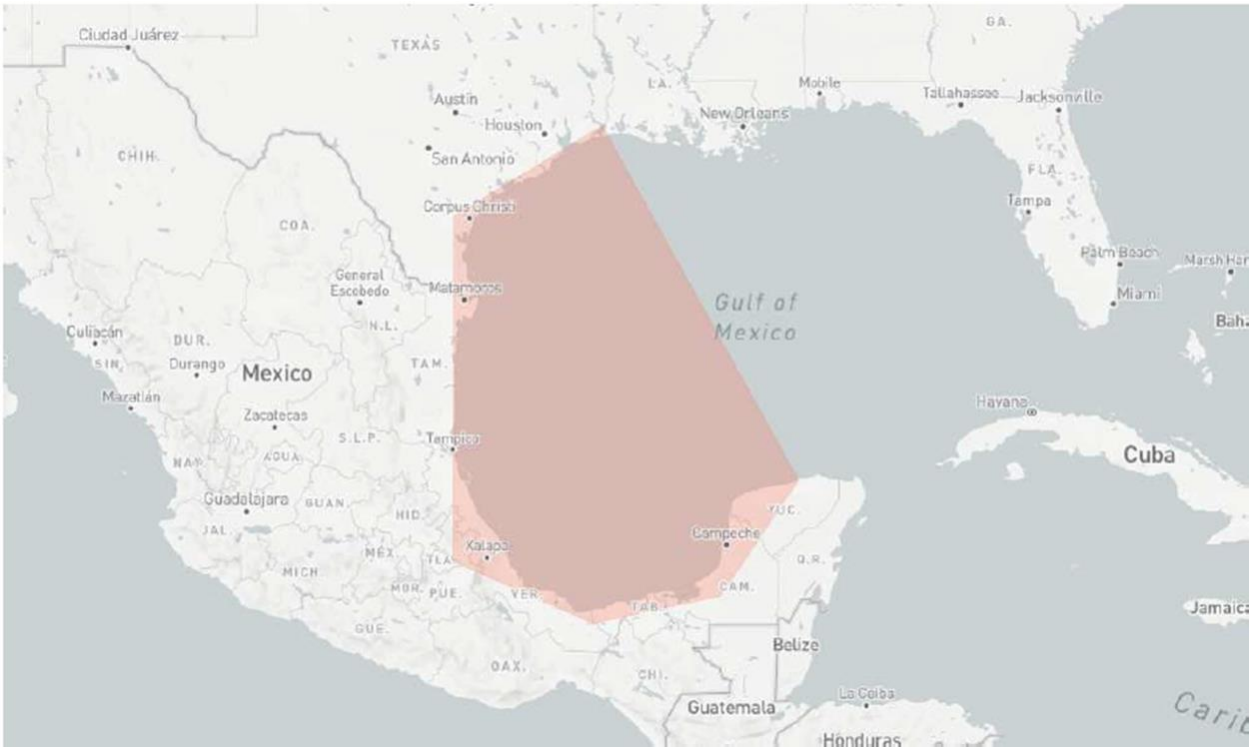

Figure 2. Red polygon denotes the region used to determine whether named storms impacted either the seed bank region for K. brevis (Bay of Campeche) or the Texas coast.

Data Analysis

All data analyses were performed in R v 3.6.2 (R Core Team) and PRIMER v7 (Clarke and Gorley 2015).

Phytoplankton Dynamics and Environmental Drivers

The dataset used in this section was collected from August 2016 through October 2018 at the Packery Channel, Oso Inlet, Cole Park, and South Shore sites. Principal component analysis (PCA) was used to describe environmental variability in the Corpus Christi Bay system using NH_4^+, NOx, PO_4^{3-}, SiO_4, DON, DIN:Si, DIN:DIP, salinity, temperature, freshwater discharge, wind speed, U, and V. To quantify the relationships among environmental factors and phytoplankton biovolume, diatom biovolume, and dinoflagellate biovolume, pairwise Kendall's Tau correlations were conducted on untransformed data (stats v. 3.6.2; (R Core Team 2019)).

K. brevis Dynamics

Environmental data were normalized for analyses conducted in PRIMER v7 to make the scales of each variable more similar (Clark and Gorley 2015). To assess annual and interannual variability in fall environmental conditions, PCA was conducted using all available data points (n = 204) and NH_4^+, NOx, PO_4^{3-}, SiO_4, salinity, temperature, 5-day precipitation totals, wind speed, U, V, and daily discharge as environmental variables of interest (PRIMER v7). A multivariate one-way ANOSIM was used to quantify dis/similarity among all possible year pairs, with the aforementioned variables characterizing each year (PRIMER v7). To determine which variables were most likely related to the observed differences among year-pairs a SIMPER analysis was subsequently conducted (PRIMER v7).

Logistic regression (LogisticDx v 0.2) (Dardis 2015) was used to explore relationships between *K. brevis* presence/absence and environmental variables. Environmental variables of

interest were salinity, temperature, wind speed, U, V, daily precipitation, 5-day precipitation totals, and daily freshwater discharge. Nutrient data were not included in this analysis due to issues with collinearity among nutrient variables as well as with salinity. Dredge and a summary of model averages (MuMIn v 1.43.6) (Barton 2020) were used to determine the importance of each explanatory variable and the best models were built. The models were compared for relative quality using Akaike's Information Criterion (AICc) and assessed for goodness of fit using the Hosmer-Lemeshow test (LogisticDx v 0.2) (Dardis 2015). Nagelkerke pseudo R^2 values (pscl v 1.5.2) (Jackman 2020) were also calculated to assess the variability explained by each of the models and can be interpreted similarly to a traditional R^2 value (Smith and McKenna 2013; Walker and Smith 2016). Finally, the odds ratios for each variable in the final explanatory model were calculated to aid in the interpretation of the influence of each variable. For multivariate models, the odds ratio is interpreted as the likelihood of *K. brevis* presence due to a change in one variable with all other variables held constant, e.g. an odds ratio of 1.17 for variable x indicates that, with all else held constant, there is a 17% increase in the probability of a red tide occurring with each 1 unit increase in variable x.

To quantify differences in community composition between years when *K. brevis* was present but did not bloom (2017, 2018) and a year when *K. brevis* was present and reached bloom levels (2016), a more detailed analysis of phytoplankton community composition and environmental drivers during the late summer-early fall was conducted. Non-metric multidimensional scaling (nMDS) was used to visually represent the dis/similarity among phytoplankton communities between August and November of 2016, 2017, and 2018 (PRIMVER v7). A one-way multivariate ANOSIM was conducted to quantify differences in the community composition among all possible year pairs (PRIMER v7). To determine which

phytoplankton taxa were driving observed differences among year-pairs, a SIMPER analysis was subsequently conducted. Lastly, to determine how environmental variability was related to variability in community composition the BEST test (BIO-ENV procedure) was conducted with NH_4^+, NOx, PO_4^{3-}, SiO_4, salinity, temperature, 5-day precipitation totals, wind speed, U, V, and daily discharge as explanatory variables.

Results

Phytoplankton Dynamics and Environmental Drivers

PCA was used to explore temporal variability in the environmental conditions from late summer 2016 through fall 2018. The first principal component (PC1) was primarily composed of salinity, NOx, PO_4^{3-}, SiO_4, and temperature, and explained approximately 19.0% of the variability (Fig 3). This axis likely represents variability in rainfall given the inverse relationship between daily freshwater discharge and salinity observed along this PC. The contribution of temperature to this PC also indicates that precipitation and discharge tend to follow a seasonal cycle. Many of the sampling events that demonstrated variability along this axis were associated with fall sampling events, though all seasons demonstrated some variability along this axis. PC2 was primarily composed of temperature, dissolved oxygen, DON, U and V, and explained approximately 17.7% of the variability. The strong contribution of temperature and dissolved oxygen to this axis suggests that it is representative of a seasonal metabolism signal (Fig 3).

Phytoplankton biovolume demonstrated seasonal variability with median phytoplankton biovolume highest in the spring and lowest in the winter (Fig. 4). Diatom and dinoflagellate biovolume also demonstrated seasonal variability. Median diatom biovolume was higher during spring and winter than summer and fall, opposite of the pattern in dinoflagellate biovolume (higher during the summer and fall than during the spring and winter). At finer temporal

resolution, peaks in total phytoplankton biovolume and diatom biovolume during the spring frequently followed the occurrence of low salinity (high nutrient) conditions (Fig. 5). In contrast, phytoplankton tended to show a much weaker response, if any, during the fall following the occurrence of low salinity conditions.

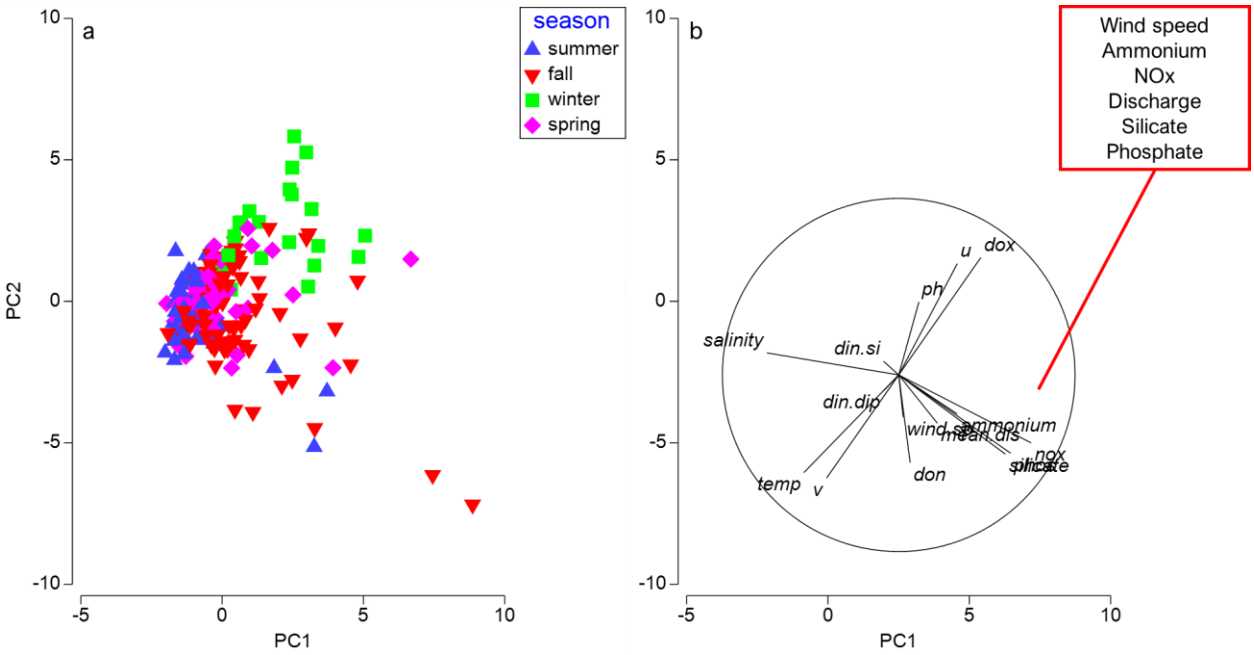

Figure 3. PCA plot with sampling events coded by season (a) and vector trajectories (b). Variable abbreviations are as follows, temperature (temp), dissolved oxygen (dox), dissolved organic nitrogen (don), nitrate + nitrite (nox), phosphate (phos), wind speed (wind.sp), freshwater discharge (mean.dis). All other variables are as displayed.

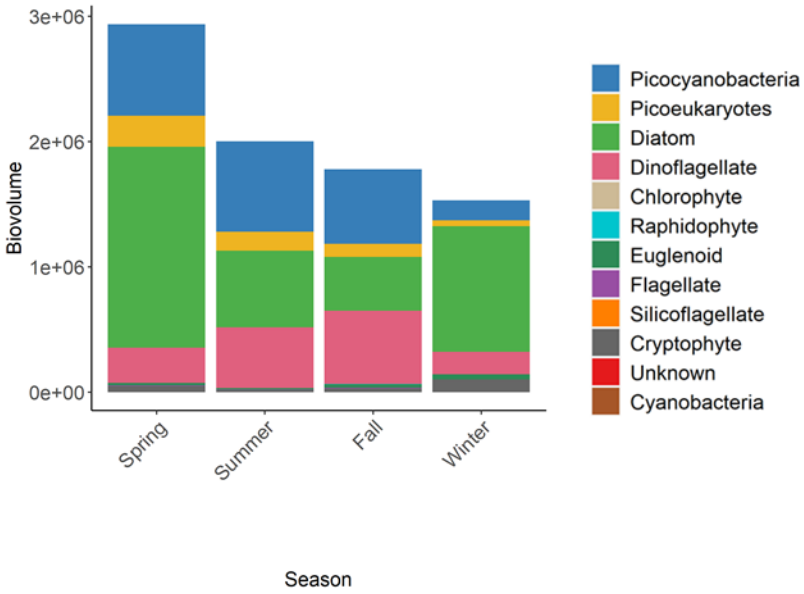

Figure 4. Stacked bar graphs of median phytoplankton biovolume (μm^3 mL^{-1}) coded by major taxonomic group.

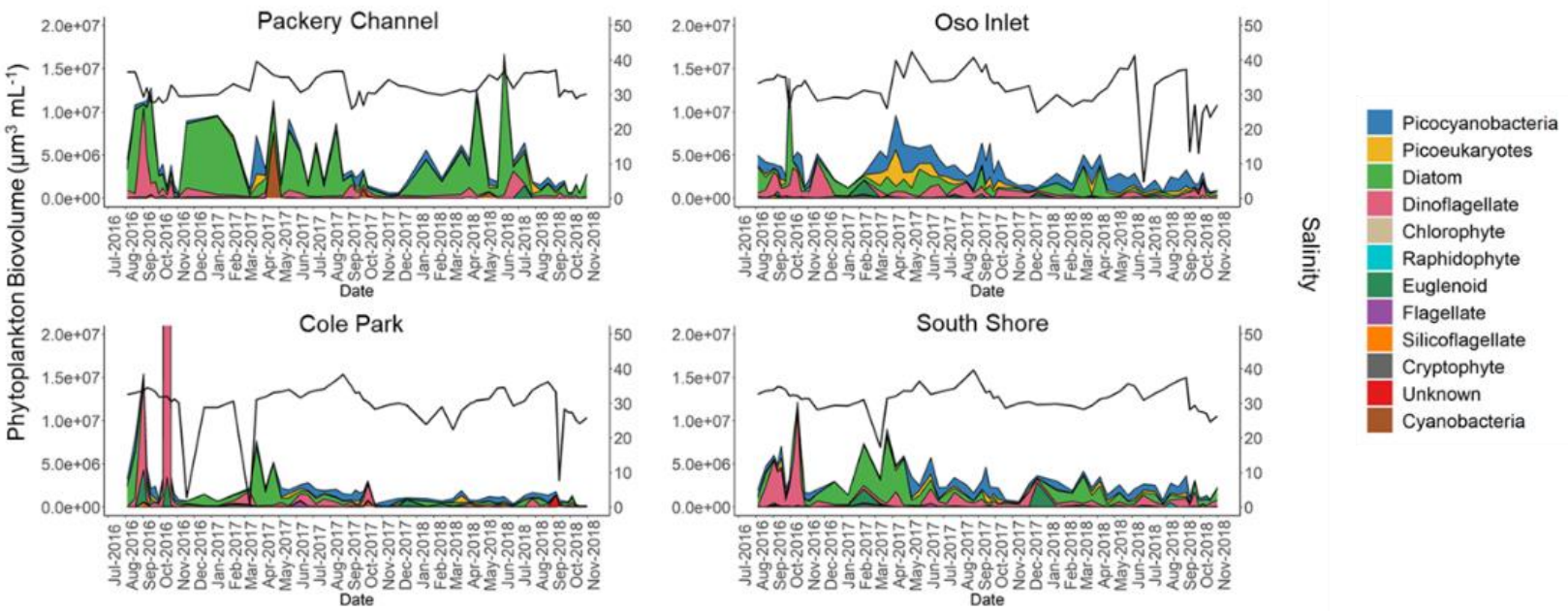

Figure 5. Temporal variability in phytoplankton biovolume (µm^3 mL^{-1}) and major group contribution at all sites studied. Black line represents salinity. At Cole Park, the sampling event with phytoplankton biovolume greater than the scale of the plot was on 10/14/2016 associated with a K. brevis red tide. The total biovolume was 1.94 x 10^8 µm^3 mL^{-1}.

Results from pairwise Kendall's Tau correlations indicated that phytoplankton biovolume was inversely correlated with NOx, PO_4^{3-}, and SiO_4 and positively correlated with temperature, pH, and salinity (Table 3). Diatom biovolume was inversely correlated with NOx, PO_4^{3-}, SiO_4, and DON, while dinoflagellate biovolume was inversely correlated with NOx, NH_4^+, DIN:Si, DIN:DIP, and wind speed.

Table 3. Environmental variables found to be significantly ($p < 0.05$) related to total phytoplankton biovolume, diatom biovolume, and dinoflagellate biovolume based on pairwise Kendall's Tau correlations. Inverse correlations are bolded.

Variables	Correlation with Biovolume	Correlation with Diatoms	Correlation with Dinoflagellates
NOx	**-0.236**	**-0.219**	**-0.153**
PO_4^{3-}	**-0.139**	**-0.216**	-
SiO_4	**-0.229**	**-0.411**	-
NH_4^+	-	-	**-0.202**
DON	-	**-0.161**	0.156
DIN:Si	-	0.188	**-0.238**
DIN:DIP	-	0.119	**-0.170**
Temperature	0.095	-	0.218
pH	0.232	-	0.220
Salinity	0.215	-	0.084
Wind Speed	-	0.244	**-0.135**

K. brevis Dynamics

K. brevis was detected in the Corpus Christi Bay system during sampling in 2016, 2017, and 2018, but was not detected during sampling in 2019 and 2020. Bloom levels of *K. brevis* were only detected during 2016 (Table 4). The number of named storms affecting the Western GoM was highest in 2020, followed by 2017 and 2019, then 2016, while 2018 had no named storms.

Table 4. Karenia brevis presence/absence and bloom condition from 2016 – 2020.

Year	Red Tide[+]	First Observed	Last Observed	Named Storms[*]	Annual and Fall Precipitation (cm)
2016	Y – B	9/02	11/18	2 (0, 2)	83.20; 25.27
2017	Y – NB	8/11	10/19	4 (1, 2)	82.03; 26.31
2018	Y – NB	9/12	11/7	0	129.19; 74.42
2019	N	-	-	4 (1, 0)	67.58; 23.45
2020	N	-	-	6 (2, 4)	66.20; 12.13

[+] Y-B is present-bloom; Y-NB is present-no bloom; N is no bloom.
[*] The number outside of parentheses indicates total no. of storms, the first number inside parentheses is the no. of storms that made landfall on the TX coast, and the second number inside parentheses is the no. of storms that affected the Southern Gulf of Mexico.

To explore environmental variability among these five years, a PCA was conducted. The first principal component (PC1) was primarily composted of PO_4^{3-}, SiO_4, salinity, and NOx and explained approximately 28.3% of the variability (Fig. 6). Similar to findings from the 2016-2018 PCA (Fig. 3), this axis likely represents rainfall variability. Sampling events from the year 2018 demonstrated the greatest variability along PC1, though other years demonstrated some variability along this axis. PC2 was primarily composed of U, V, temperature, and wind speed and explained approximately 18.5% of the observed variability. This axis likely represents variability in the direction and magnitude of wind from late summer through fall as well as the decrease in temperatures from late summer through to late fall. Sampling events from all five years tended to demonstrate a similar degree of variability along this axis, in contrast to that observed for PC1.

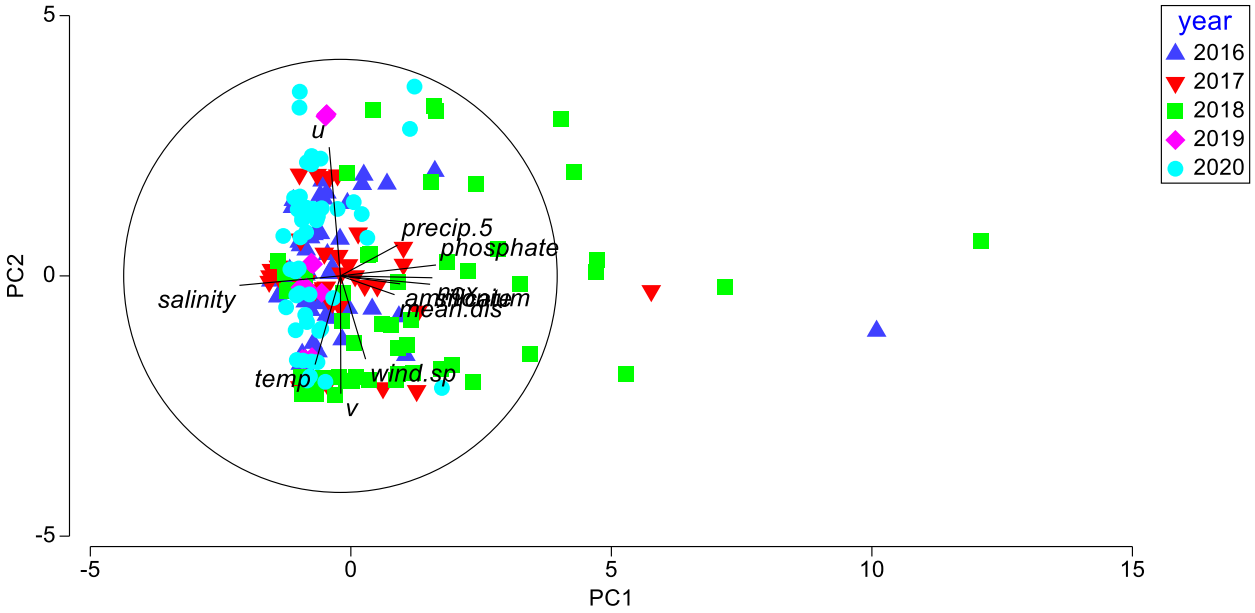

Figure 6. Principal component analysis of all late summer-fall sampling events from 2016-2020 with sampling events coded by year.

Results from multivariate one-way ANOSIM testing revealed significant differences among years (Table 5). All year-pairs demonstrated significant differences, except for comparisons including the year 2019, though many of the significant comparisons were accompanied by a relatively low R statistic, indicating a large degree of overlap in environmental conditions. The two year-pairs that demonstrated the lowest degree of overlap (highest R statistic) were 2016-2018 and 2018-2020. The follow-up SIMPER analysis indicated that increased precipitation during 2018 and associated changes in salinity and inorganic nutrient concentrations drove much of the observed interannual variability (Table 6). Other variables that demonstrated importance were wind speed, U, V, and temperature.

Table 5. Results of a one-way ANOSIM comparing environmental conditions among years. Significant comparisons are bolded. The variables used to characterize each year were NH_4^+, NOx, PO_4^{3-}, SiO_4, salinity, temperature, 5-day precipitation totals, wind speed, U, V, and daily discharge.

Groups	R Statistic	P value
2016, 2017	**0.058**	**0.010**
2016, 2018	**0.155**	**0.001**
2016, 2019	0.081	0.204
2016, 2020	**0.056**	**0.001**
2017, 2018	**0.063**	**0.012**
2017, 2019	-0.034	0.600
2017, 2020	**0.051**	**0.014**
2018, 2019	-0.077	0.746
2018, 2020	**0.167**	**0.001**
2019, 2020	0.101	0.128

Table 6. Median and (range) of selected variables from August thru November of each study year. Precipitation is the only variable presented as total for the period of August thru November of each study year, though 5-day precipitation totals were used in the SIMPER analysis. Results of SIMPER analysis are indicated with superscript letters (a > b > c…).

Year	2016	2017	2018	2019	2020
Discharge ($ft^3\ s^{-1}$)	126.17^{b} (46.8 - 682.44)	86.01^{b} (39.93 - 456.94)	2171.15^{a} (105.1 - 8694.07)	85.07^{b} (46.2 - 157.98)	120.82^{b} (83.51 - 494.73)
Precipitation (cm)	25.27^{b}	$26.31^{b,c}$	74.42^{a}	23.45^{c}	$12.13^{b,c}$
Wind Speed ($m\ s^{-1}$)	5.56^{c} (3.05 - 9.70)	6.35^{b} (3.10 - 9.01)	7.48^{a} (3.14 - 8.53)	4.82^{e} (2.49 - 7.13)	5.73^{d} (3.58 - 8.61)
U ($m\ s^{-1}$)	-3.67^{b} (-4.73 - -0.20)	-4.72^{b} (-6.23 - -1.57)	-5.52^{b} (-7.42 - 3.56)	-3.83^{b} (-6.62 - -1.62)	-1.94^{a} (-5.77 - 4.68)
V ($m\ s^{-1}$)	1.29^{b} (-9.51 - 5.57)	-0.32^{a} (-6.61 - 7.18)	$1.54^{a,b,c}$ (-6.31 - 5.83)	1.65^{a} (-1.24 - 2.37)	-0.66^{c} (-6.57 - 6.51)
Salinity	32.26^{a} (2.79 - 36.57)	32.85^{a} (25.85 - 40.78)	29.12^{b} (3.86 - 37.41)	$31.80^{a,b}$ (28.87 - 34.89)	35.01^{a} (30.10 - 36.65)
Temperature (°C)	29.1^{a} (22.1 - 33.1)	27.7^{b} (21.6 - 32.2)	28.4^{c} (18.4 - 30.7)	26.5^{d} (13.4 - 30.8)	27.2^{c} (15.1 - 31.7)
NH_4^+ (µM)	3.03^{b} (0.61 - 58.43)	3.63^{a} (1.37 - 33.96)	3.26^{c} (0.03 - 18.6)	0.29^{c} (0.05 - 1.54)	4.10^{a} (0.71 - 15.27)
NOx (µM)	0.60^{c} (0.02 - 50.08)	0.31^{b} (0.02 - 44.28)	0.28^{a} (0.04 - 30.26)	0.18^{d} (0.13 - 0.79)	0.60^{d} (0.17 - 20.47)
PO_4^{3-} (µM)	0.62^{b} (0.04 - 12.38)	0.87^{b} (0.13 - 5.68)	0.77^{a} (0.06 - 37.79)	0.64^{b} (0.22 - 1.06)	0.69^{b} (0.02 - 7.15)
SiO_4 (µM)	38.33^{b} (3.92 - 89.69)	52.56^{b} (6.49 - 141.05)	76.57^{a} (10.89 - 432.13)	45.59^{b} (26.37 - 71.07)	43.09^{b} (7.68 - 136.45)

Modeling indicated that warmer, lower salinity conditions were associated with the presence of *K. brevis* (Table 7). Further modeling work with *K. brevis* abundance data from 2016-2018 indicated that salinity, temperature, discharge, and U were related to *K. brevis* abundance (Table 8). The relationship with salinity was non-linear, with relatively low abundances associated with salinity less than 25 and salinity greater than 35 (Fig. 7).

Table 7. Results from final logistic regression model explaining red tide presence/absence from August through November of 2016 through 2020.

Dataset	Explanatory Variables	Estimates	Estimate Standard Error	95% Confidence Interval	Odds Ratio	Nagelkerke Pseudo-R^2
Presence/Absence 2016-2020	Temperature	0.194	0.126	-0.021, 0.476	1.214	0.27
	Salinity	-0.286	0.103	-0.517, -0.109	0.751	

Table 8. Results from final explanatory model explaining red tide abundance between August and November of 2016, 2017, and 2018.

	Linear Variables			
Abundance 2016-2018	Explanatory Variables	Estimates	Standard Error	Adjusted R^2
	Temperature	0.198	0.154	0.51
	U	-0.765	0.244	
	Discharge	-0.003	0.001	
	Smoothed Variables			
	Explanatory Variables	Polynomial	P-value	
	Salinity	4.414	0.001	

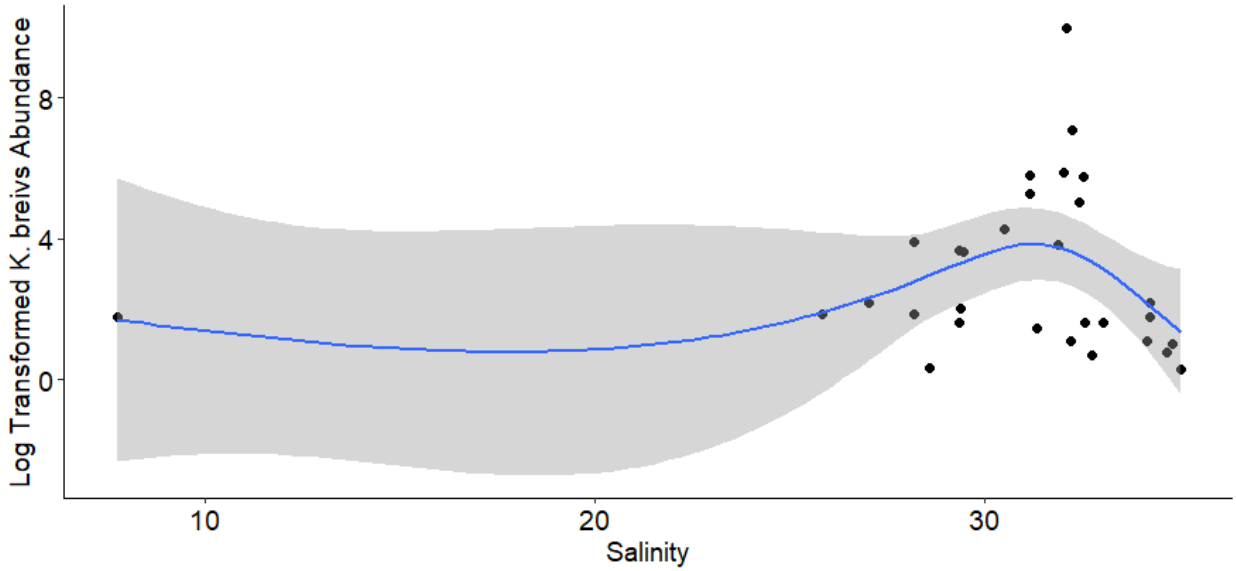

Figure 7. Visual representation of the smooth fitted to salinity in the final model explaining K. brevis abundance. The blue line represents model output and the grey shaded area represents confidence intervals. The points are actual data points.

To assess variability in phytoplankton community composition among the late summer-fall of 2016, 2017, and 2018 nMDS, ANOSIM testing, and a SIMPER analysis were performed. Results from nMDS indicated that communities from the fall of 2016 tended to be more closely related than to those from either 2017 or 2018 (Fig. 8). Communities in 2017 and 2018 demonstrated more variability within each year and a greater degree of overlap between the two years. Results from a one-way multivariate ANOSIM supported the nMDS results. All years demonstrated significantly different phytoplankton communities than all other years (Table 9), though the degree of dissimilarity was different for each year comparison. The highest R statistic of the year-pairs was found for 2016-2018 at 0.480, though the R statistic for the 2016-2017 comparison also indicated a relatively large degree of dissimilarity (R statistic = 0.393). The relatively low R statistic of the 2017-2018 comparison (0.176) supported the greater degree of overlap observed between these years in the nMDS results (Fig. 8).

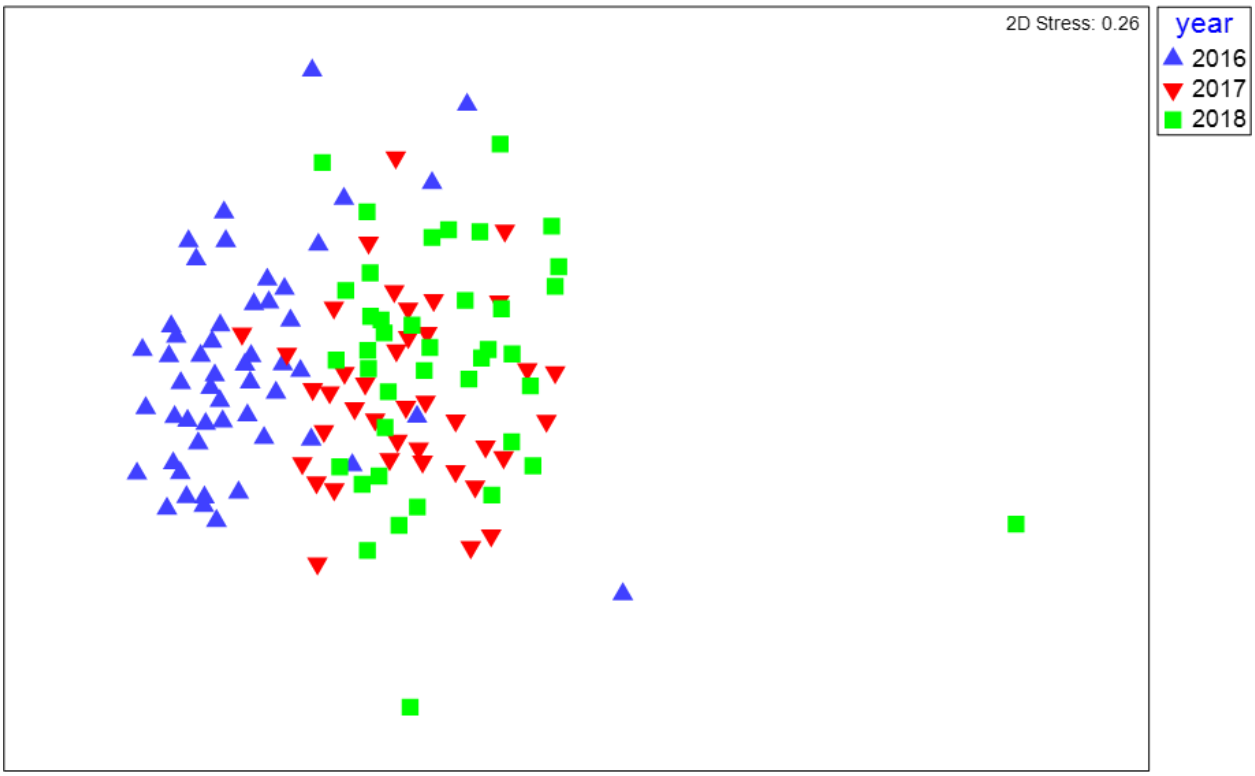

Figure 8. Non-metric multidimensional scaling of phytoplankton community composition with each sampling event coded by year.

Table 9. Results of a one-way ANOSIM comparing phytoplankton community composition among years.

Groups	R Statistic	P value
2016, 2017	0.393	0.001
2016, 2018	0.480	0.001
2017, 2018	0.176	0.001

A follow-up SIMPER analysis indicated that phytoplankton communities during 2016 was generally characterized by increased importance of dinoflagellate genera (*Karenia*, *Prorocentrum*, *Scripsiella*, *Ceratium*, *Cochlodinium*, *Protoperidinium*, *Pyrdoinium*, and *Gonyaulax*), whereas 2017 and 2018 were characterized by increased importance of diatom genera (*Pseudonitzschia*, *Leptocylindrus*, *Rhizosolenia*, and *Asterionella*) (Fig. 9). Fall communities in 2018 were additionally characterized by increased importance of small *Pyramimonas*-like organisms, though they were never a dominant biovolume contributor. Lastly,

phytoplankton community composition was compared to a suite of environmental parameters using the BEST test (BIO-ENV procedure). The best combination of variables explaining community composition variability included PO_4^{3-}, SiO_4, and mean discharge and had a correlation coefficient of 0.234.

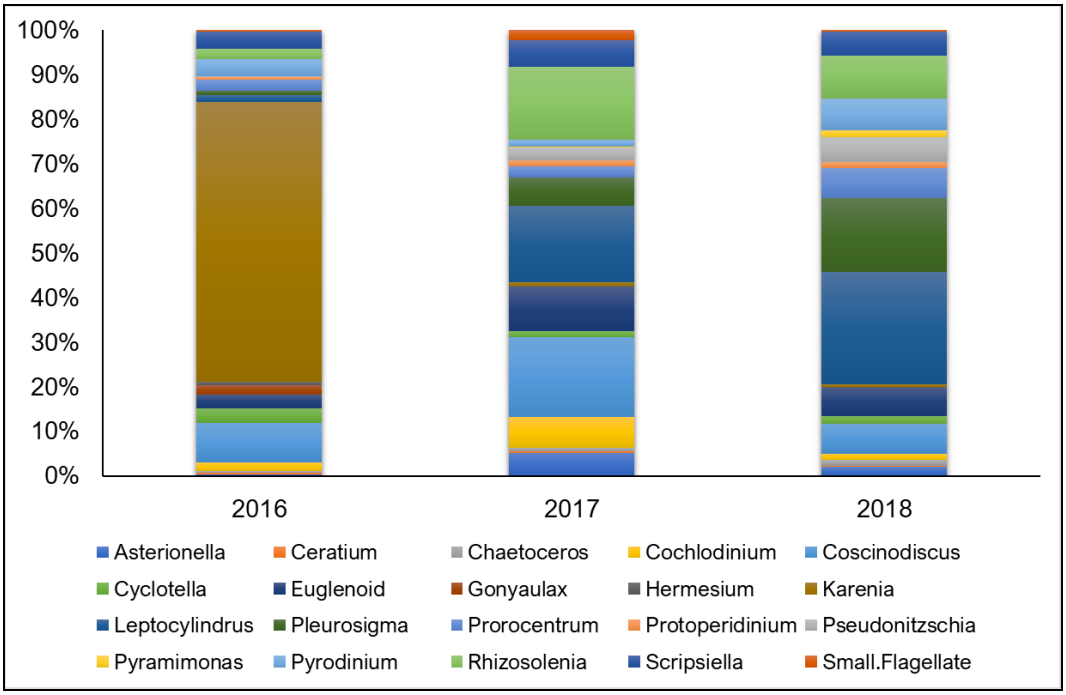

Figure 9. Stacked bar graph showing the relative contribution of the top 20 genera contributing to observed year-to-year variability identified using the SIMPER analysis.

Discussion

Phytoplankton Dynamics and Environmental Drivers

Phytoplankton in the Corpus Christi Bay system demonstrated a unimodal pattern in total community biovolume, with maximum biovolume observed during the spring and minimum biovolume observed during the winter. This pattern in phytoplankton biovolume has been observed in other Texas estuaries and is the most common pattern observed across the world (Pinckney et al. 1998; Cloern and Jassby 2010; Guinder et al. 2010; Baek et al. 2015; Reyna et al. 2017; Chin 2020; Nohe et al. 2020; Cira et al. 2021). Phytoplankton biovolume was inversely related to nutrients and positively related to temperature, pH, and salinity. These findings,

combined with observations that precipitation-driven declines in salinity (nutrient inputs) were associated with peaks in phytoplankton biovolume during spring but not during fall or winter, indicate that phytoplankton in Corpus Christi Bay are not exclusively limited by nutrients throughout the year.

Precipitation events (single day rainfall total > 0.25 cm) were more common during fall than spring (58 vs 37) and precipitation totals tended to be higher during fall (mean fall total 2016-2018 = 33.99 cm) than during spring (mean spring total 2016-2018 = 25.06 cm). Phytoplankton washout due to increased riverine inflows and stormwater runoff may have been more common during the fall than during the spring, acting to limit phytoplankton growth response to added nutrients (Dorado et al. 2015; Reyna et al. 2017; Chin 2020; Cira et al. 2021). Additionally, dinoflagellates tended to contribute a larger proportion of biovolume to the phytoplankton community during fall than during spring and were also positively correlated with salinity. Dinoflagellates tend to be more susceptible to losses due to washout than diatoms and other fast-growing taxa, supporting observations of less phytoplankton growth following washout during the fall (Roelke et al. 2013; Dorado et al. 2015). Phytoplankton growth rates did respond to nutrient additions during an experiment conducted with water from the South Shore site in October 2017 (Tominack 2021), indicating that phytoplankton are nutrient limited during this period despite lack of observed growth following precipitation events, lending further support to the importance of other factors such as flushing that limit phytoplankton growth during the fall.

During the winter, low temperatures most likely acted to limit phytoplankton growth despite higher ambient nutrient concentrations. Temperature limitation of phytoplankton has been demonstrated in numerous estuaries, both observationally and experimentally (Cloern et al.

1999; Fisher et al. 1999; Lomas and Glibert 1999; Örnólfsdóttir et al. 2004; Cira et al. 2016). Additionally, phytoplankton growth rates did not respond to nutrient additions during an experiment conducted with water from the South Shore site in January 2018, further supporting a role for temperature in limiting winter phytoplankton growth in Corpus Christi Bay (Tominack 2021). Despite the relatively low phytoplankton biovolume observed during the winter, however, diatom biovolume tended to be higher during the winter than during the summer and fall. This is well in line with known preferences of diatoms for cooler temperatures and high ambient nutrient conditions (Holland et al. 1975; Cloern et al. 1999; Cloern and Dufford 2005; Suggett et al. 2009; Baek et al. 2015).

In contrast, phytoplankton during spring and summer appear to be most strongly limited by nutrient availability. Release from light and temperature limitation in early spring is often related to the success of spring phytoplankton blooms (Sverdrup 1953; Pinckney et al. 1998; Winder and Sommer 2012; Nohe et al. 2020), with nutrients becoming the dominant factor limiting phytoplankton growth. Ambient nutrient concentrations tended to be lower during the spring than during the fall, indicating that as temperature and light are no longer limiting phytoplankton growth, the nutrient pool is drawn down and becomes limiting. The ability of diatoms to rapidly respond to changing environmental conditions and favorability under turbulent conditions were likely a key factor leading to the dominance of diatoms during the spring (Cloern and Dufford 2005; Suggett et al. 2009; Baek et al. 2015). Despite being characterized by relatively low concentrations of inorganic nutrients, summer conditions supported relatively high phytoplankton biovolume. This was most likely related to the high capacity of shallow lagoonal systems, such as Corpus Christi Bay, for internal nutrient cycling and regeneration (Pinckney et al. 2001; Glibert et al. 2005; Geyer et al. 2018). Heavy reliance on

recycled nutrients, combined with warmer temperatures and decreased precipitation during this period likely also acted to facilitate the observed increase in dinoflagellate biovolume during the summer (Paerl and Justić 2013; Paerl et al. 2014; Baek et al. 2015; Dorado et al. 2015; Glibert et al. 2016; Shangguan et al. 2017). Under current conditions, these dynamics can be represented by a simple conceptual diagram (Fig. 10).

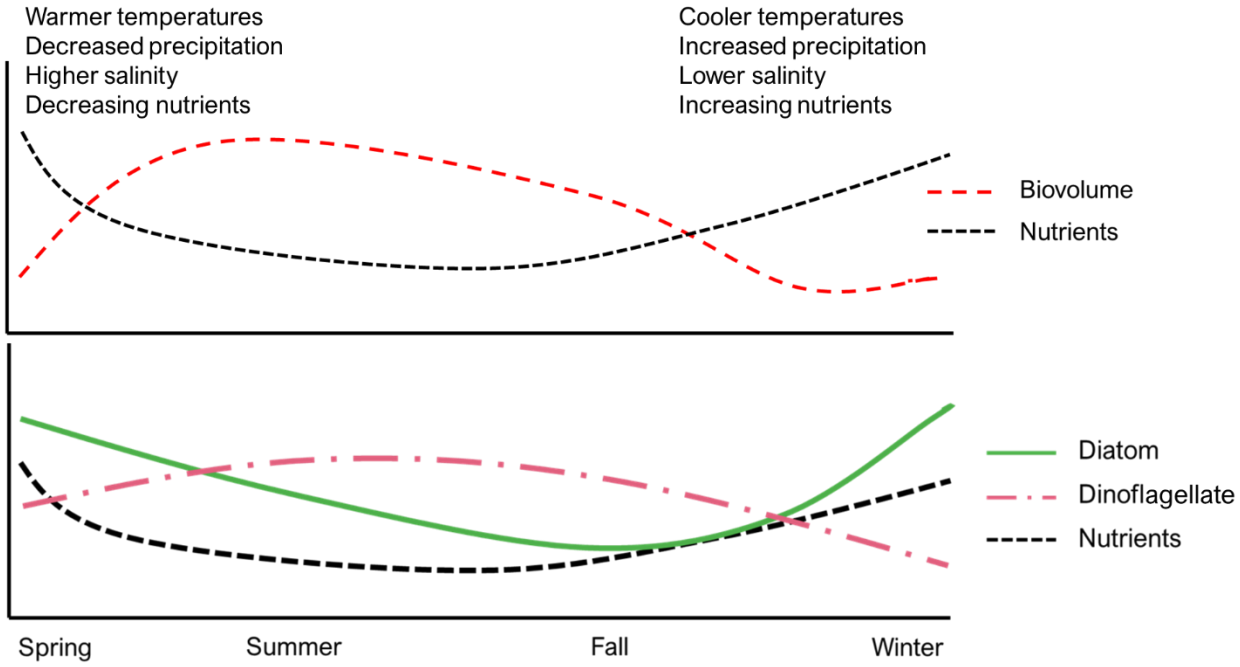

Figure 10. Conceptual diagram of current phytoplankton-environment dynamics in Corpus Christi Bay, Texas.

Future projections of climate change indicate that the South Texas coast is likely to experience warmer and drier conditions overall, punctuated by extreme precipitation events (Pachauri et al. 2014; Nielsen-Gammon et al. 2020; U.S. Census Bureau). As conditions warm, it could be expected that the spring phytoplankton bloom will occur earlier, as has been observed in other systems (Nohe et al. 2020). Due to relatively low inflow in the Corpus Christi Bay system, an earlier spring bloom has the potential to result in an earlier and more rapid depletion of inorganic nutrient pools and potentially an earlier shift to increased dinoflagellate biovolume. As drier conditions become more common there is likely to be even less freshwater inflow into

Corpus Christi Bay than currently, leading to increases in salinity and residence times throughout the system. Results from the PCA showed that inorganic nutrients concentrations were related to freshwater discharge, indicating that reduced inflow could shift Corpus Christi Bay phytoplankton to a stronger reliance on recycled N (typically in reduced form), conditions that tend to favor dinoflagellates over diatoms (Ferreira et al. 2005; Glibert et al. 2005; Altman and Paerl 2012; de Souza et al. 2014). Additionally, dinoflagellates tend to be more successful in systems with longer residence times and lower rates of flushing (Bricker et al. 2008). Though dinoflagellates can be a healthy food source for consumers (rich in DHA) there are proportionally more harmful algal bloom formers in this taxonomic group when compared to diatoms (Cloern and Dufford 2005; Paerl and Justić 2013), indicating that there may be increased potential for the occurrence of HABs in general. Under future climate scenarios there is then potential for altered food web dynamics due to shifts in the timing of the spring bloom, changes in community composition, and potential increase in HAB occurrence. Potential changes to the current observed phytoplankton dynamics under future climate scenarios (Fig. 11) can be compared to current conditions (Fig. 10).

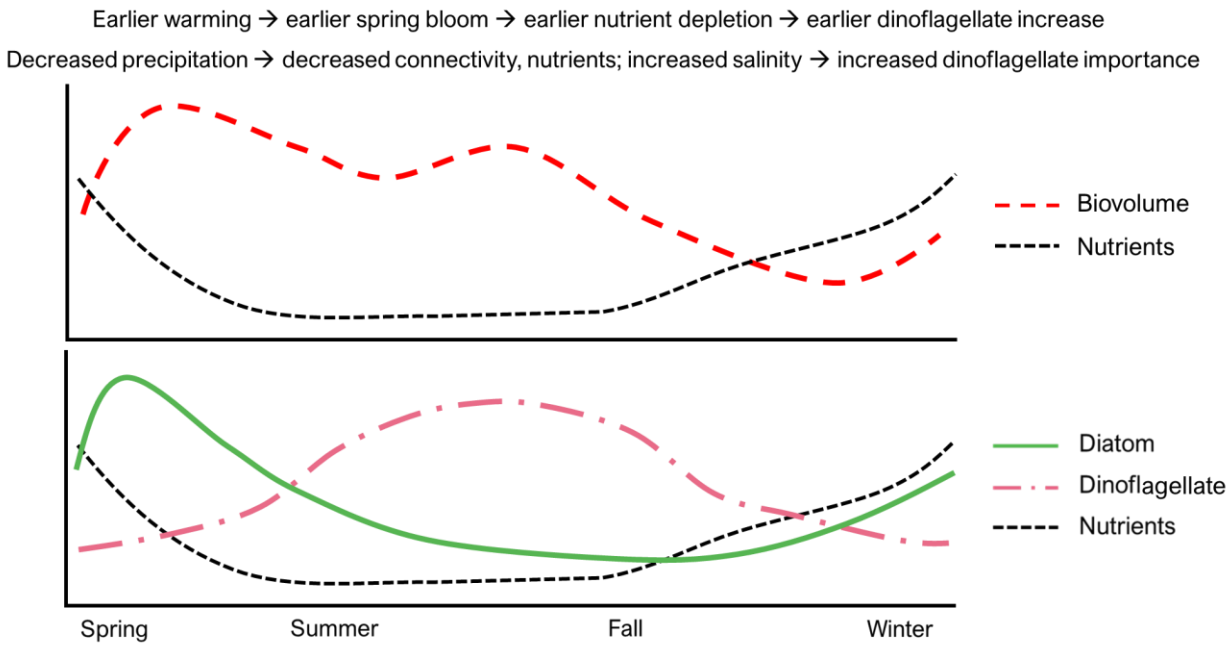

Figure 11. Conceptual diagram of future phytoplankton-environment dynamics in Corpus Christi Bay, Texas

K. brevis Dynamics

Historically, *K. brevis* red tides occurred relatively infrequently on the TX coast, though since approximately 1995 the frequency of occurrence has increased, and red tides are now a near-annual occurrence (Magaña et al. 2003; Tominack et al. 2020). In the Nueces Estuary, salinity (+), the El Niño Southern Oscillation (-; ENSO), and the North Atlantic Oscillation (-; NAO) were related to the occurrence of red tides (Tominack et al. 2020). This indicates that 1) conditions within the estuary are important in determining the success of red tides and 2) long-term increases in salinity throughout much of the system (Bugica et al. 2020) and periodic ENSO-driven precipitation have interactive effects in supporting or discouraging blooms of *K. brevis* within Nueces Estuary. As mentioned in the discussion of phytoplankton dynamics, future climate projections indicate warmer and drier conditions in the Corpus Christi Bay region. Based on the results from Tominack et al. (2020), resulting higher salinities have the potential to increase the prevalence of conditions conducive to *K. brevis* red tides.

The current study investigated *K. brevis* dynamics at a finer temporal scale to better understand factors that may support or fail to support a red tide in Corpus Christi Bay. *K. brevis* was detected in Corpus Christi Bay during the fall of 2016, 2017, and 2018, and reached levels when discolored water becomes apparent (> 100,000 cells L^{-1}; Tester and Steidinger 1997; Steidinger 2009) for approximately two weeks during 2016. During the fall of 2019 and 2020 no *K. brevis* cells were detected during routine sampling. Study years can therefore be classified as present-bloom (PB), present-no bloom (P), and absent (A). Multivariate analyses comparing environmental conditions among years were employed to determine if there were any specific environmental factors that could be used to distinguish among years and related to the three potential *K. brevis* conditions.

Results from the PCA indicated that El Niño-driven precipitation during 2018 and associated decreases in salinity and increases in inorganic nutrients drove much of the observed variability in environmental conditions. El Niño conditions have previously been shown to be tightly coupled with salinity variability in Texas estuaries (Tolan 2007) and inversely related to the occurrence of *K. brevis* red tides in the Nueces Estuary (Tominack et al. 2020). It is therefore most likely that these conditions were instrumental in preventing the *K. brevis* cells present during 2018 from accumulating to bloom levels. Prior to prolonged heavy rainfall beginning 9/10/18 (8-day total = 38.93 cm) there was at least one localized report of discolored water and dead fish in Corpus Christi Bay (Wetz, personal obs.), along with reports of *K. brevis* along the coast, though following this precipitation event *K. brevis* was only detected in relatively low abundances during routine sampling. These observations lend further support to the lack of bloom development due to physical removal from the system and potentially inhospitable salinity conditions (*K. brevis* optimum ~30-35; mean salinity 9/21/18 thru 11/7/18 = 25.97).

Additional support for the role of decreasing salinity comes from the *K. brevis* modeling results. The observed relationship between *K. brevis* abundance and salinity was non-linear with relatively low abundances observed and salinities below ~27 and above ~35. This indicates that although *K. brevis* was present, decreasing salinity was negatively associated with the success of *K. brevis*. This dynamic also aids in the interpretation of the inverse relationship between salinity and *K. brevis* presence during the period from 2016 through 2020. In Corpus Christi Bay, salinity conditions oscillate between within the optimum range for *K. brevis* and below the optimum range for *K. brevis* less frequently (less than 10% of data points with salinity < 25) than in the opposite direction, salinity above the optimum range for *K. brevis* (20% of data points with salinity > 35). The relationship between *K. brevis* and salinity is, therefore, more nuanced than previously thought, especially in low inflow estuaries strongly influenced by individual precipitation events. These results represent a critical first step toward understanding the role of salinity and precipitation in driving *K. brevis* dynamics in an estuarine setting.

Interestingly, the PCA yielded no other clear patterns in environmental variability differentiating among the years 2016, 2017, 2019, and 2020. There were, however, subtle differences among these years based on results from the one-way ANOSIM and SIMPER analysis. The year 2016 was found to be significantly different from 2017 and 2020, though there was still a large degree of similarity as determined by the relatively low R statistics (0.058 and 0.056, respectively). The fall of 2016 tended to have lower inorganic nitrogen (NH_4^+ and NOx), warmer temperatures, lower overall wind speeds, and stronger northern winds than 2017. Despite the lack of precipitation, freshwater discharge, and salinity as important factors differentiating these years, the watershed derived nature of NOx suggests there was a difference in freshwater dynamics not fully captured by this dataset. Indeed, salinity decreased and NOx concentrations

increased following Hurricane Harvey (landfall 8/25/17), though the decrease in salinity was not as pronounced as that observed in September 2018. *K. brevis* had been detected prior to Hurricane Harvey and remained present at background levels until mid-October. The flushing, decreased temperatures, and increased ambient concentrations of inorganic nitrogen likely acted to physically remove *K. brevis* (via flushing) and/or favor other taxa (via decreased temperatures, increased nutrients).

Further evidence for the role of precipitation, freshwater inflows, and ambient nutrient concentrations in discouraging the formation of a red tide was found in the phytoplankton community analyses. In 2016 the phytoplankton community tended to be dominated by dinoflagellates, even before the observation of *K. brevis* in the estuary. In contrast, phytoplankton communities during the late summer-fall of 2017 and 2018 tended to have a higher contribution from diatoms, particularly *Pseudonitzschia*, *Leptocylindrus*, *Rhizosolenia*, and *Asterionella*. Modeling and experimental studies have demonstrated that pulsed nutrient inputs tend to favor diatoms over dinoflagellates, especially when SiO_4 is in ample supply (Roelke et al. 1997; Roelke et al. 1999; Tominack 2021). Results from the one-way ANOSIM comparing community composition indicated that although the communities in 2017 and 2018 were significantly different there was still a relatively large degree of similarity, whereas comparisons between those two years and 2016 indicated a relatively large degree of dissimilarity. These variations were driven by changes in PO_4^{3-}, SiO_4, and freshwater discharge. Given observed differences here, opposing conditions found to support diatoms and dinoflagellates throughout the year, and observations of these dynamics in other systems around the world (Cloern 1999; Örnólfsdóttir et al. 2004; Cloern and Dufford 2005; Cloern and Jassby 2008; Cloern and Jassby 2010; Paerl et al. 2010; Nohe et al. 2020), it is most likely that

precipitation-driven changes in freshwater inflow and nutrient delivery negatively impacted the success of dinoflagellates and allowed diatoms to outcompete *K. brevis*.

When compared to the fall of 2020, 2016 demonstrated higher wind speeds, temperature, NOx, stronger northern and eastern winds, and lower NH_4^+. Similarly, 2017 demonstrated higher wind speed, temperature, NOx, and stronger northern and eastern wind speeds than 2020. These results indicate that conditions within Corpus Christi Bay, as well as transport from offshore to inshore, should have been hospitable to *K. brevis* during 2020 (i.e., similar salinity, no difference or higher NH_4^+, lower NOx), but there was no detectable *K. brevis*. The lower NOx in 2020 compared to 2016 and 2017 indicates that freshwater inputs were likely limited and that diatoms likely would not have had a competitive advantage over dinoflagellates. Additionally, weaker E-NE (downcoast) winds, as observed in 2020 compared to 2016 and 2017, have been shown to be critical in the induction of Ekman transport of *K. brevis* biomass from the offshore to coastal environments (Thyng et al. 2013; Henrichs et al. 2015). Despite apparent hospitable conditions for transport to and survival in the estuarine environment in 2020, no *K. brevis* was observed during sampling. It is likely that the active hurricane season of 2020 disrupted the first stage of *K. brevis* bloom initiation (accumulation in the offshore environment) in the southern and/or central GoM. A total of six named storms (includes tropical storms and hurricanes) traveled through the western and southern GoM during with four of these directly impacting the southern GoM region thought to be a seed bank for *K. brevis* and two directly impacting the TX coast. This relatively large number of storms in regions where physical mechanisms are important for the concentration of *K. brevis* and movement shoreward may have acted in myriad ways to negatively impact the formation of *K. brevis* red tides. Factors such as wind speed, region of formation/impact, timing of storm, total number of storms, and severity of storms (tropical storm

vs. hurricane) likely all play a role in how *K. brevis* dynamics are affected by extreme tropical weather. Unfortunately, this study did not assess the role of transport directly, but these findings provide evidence that understanding transport mechanisms of *K. brevis* throughout the GoM will be critical for predicting future *K. brevis* occurrences in the estuarine environment.

Conclusions

Environmental conditions were found to have the potential to support or discourage the formation of *K. brevis* red tides once biomass arrives within a system. In Corpus Christi Bay, environmental conditions that tend to favor diatoms (i.e., high inflow, decreased salinity, increased nutrients, cooler temperatures) over dinoflagellates were found to discourage the formation of a high biomass red tide despite the presence of *K. brevis*. The relationship with salinity, however, was found to be more nuanced than previously thought. Salinity within the Corpus Christi Bay system was found to exceed the optimum range of *K. brevis* more frequently (> 35 20% of the time) than it was found to be below the salinity barrier proposed in the literature (< 24 ~8% of the time). This indicates that to predict and manage the occurrence of *K. brevis* red tides it will be critical to better understand the role salinity and discharge play in supporting or discouraging red tide formation.

This study also highlights the importance of physical transport mechanisms in delivering *K. brevis* biomass to the South TX coast. It has been hypothesized that there may be estuarine seed banks for *K. brevis* along the TX coast, though there is little evidence that supports or fails to support this hypothesis. This study provides an in depth look at the presence of *K. brevis* in Corpus Christi Bay, where frequent occurrences of *K. brevis* have been documented. The lack of observed *K. brevis* cells during the late summer-fall of 2020 despite generally hospitable

conditions within the estuary supports a strong role for physical transport of *K. brevis* from seed banks located elsewhere within the GoM.

Task 2: Nutrient and salinity effects on *Karenia brevis* growth

Introduction

Many studies have been conducted to understand how specific environmental factors influence *Karenia brevis* bloom development and maintenance (Aldrich and Wilson 1960; Magaña and Villareal 2006). For instance, Aldrich and Wilson (1960) found the optimum salinity range for *K. brevis* growth and maintenance is between 27 and 37, with reduced growth and survival being noted in lab experiments conducted at salinities outside of its optimal range (Aldrich and Wilson 1960; Magaña and Villareal 2006; Maier Brown et al 2006). Aside from salinity, nutrient availability is another important factor in controlling *K. brevis* growth, but it has several life history traits that allow it to outcompete other phytoplankton for nutrients at times. For example, Sinclair and Kamykowski (2008) found that it can swim to the sediment surface to access nutrients when nutrients are scarce in the water column. *K. brevis* can also utilize a broad range of nutrient forms from a variety of sources including *Trichodesmium*-derived nitrogen (Walsh 2006), nutrients from dead fish (Steidinger 2009), stormwater runoff, fertilizer, and wastewater effluent (Vargo 2009; Heil et al. 2014), and even by grazing on *Synechococcus* (Glibert et al., 2009).

Given the complex nature of coastal waters, it is virtually certain that the interaction between environmental factors (such as salinity, nutrients, temperature, etc.) will determine the potential for bloom development. The goal of this task was to begin to understand the interactive effects of salinity and nutrients from different sources on the growth *K. brevis.* Much work has already been done in offshore waters where salinity is generally conducive to *K. brevis* growth unless influenced by irregular freshwater plumes, whereas less is known about factors contributing to bloom dynamics in estuaries. It can be expected that salinity will play a more

significant role in estuaries compared to shelf waters, and nutrient sources are expected to be more diverse than on the continental shelf. Growth experiments were conducted using salinity ranges typical of Texas estuaries, and nutrients were derived from common sources.

Methods

A strain of *Karenia brevis* was acclimated in L1 media (without silicate) to treatment salinities (25, 35) until reaching sufficient cells for experiments to begin. Treatments included a control (L1 media without nitrogen), ammonium, nitrate, fish extract, porewater and wastewater effluent. Sterilized tissue culture flasks (250 ml) were filled with 200 ml of media consisting of one of the six treatments, with three replicates for each treatment. Each treatment excluding the control had a nitrogen concentration of ~20 µM, and flasks were brought up to 200 ml with sterile-filtered seawater at the appropriate salinity. 1 ml of culture containing at least 10,000 cells per ml was added to each flask to initiate the experiment. Flasks were incubated on a 12:12 light/dark cycle using cool white fluorescent lights at a photosynthetically available radiation level of 150 µmol photons m^{-2} s^{-1} and temperature of 25ºC. Samples were collected for cell counts and preserved with Lugol's solution. An Utermohl chamber was used for enumeration on an Olympus 1X-71 inverted microscope at 20x magnification. Initially, counts were performed every other day during a lag phase, and then every day once cell growth commenced.

Results

K. brevis growth rates were highly variable over the course of the experiments. Overall, growth rates were highest in the nitrogen treatments at a salinity of 25, and much lower at a salinity of 35 (Fig. 12). At the salinity of 25, growth rates were all higher in the nitrogen treatments than the control, while there were no significant differences among nitrogen treatments. Growth in the ammonium, fish and wastewater treatments were marginally different

than in the control ($p<0.10$), but not significantly different in the porewater or nitrate treatments. At a salinity of 35, positive growth was only observed in the ammonium, wastewater and fish treatments, but growth was highly variable overall. There were no significant differences between treatments at this salinity. At the time of the preparation of this report, the research team was still trying to establish cultures at salinities of 15 and 45, emphasizing the difficulty of achieving cell growth outside of the optimal salinity window for *K. brevis*.

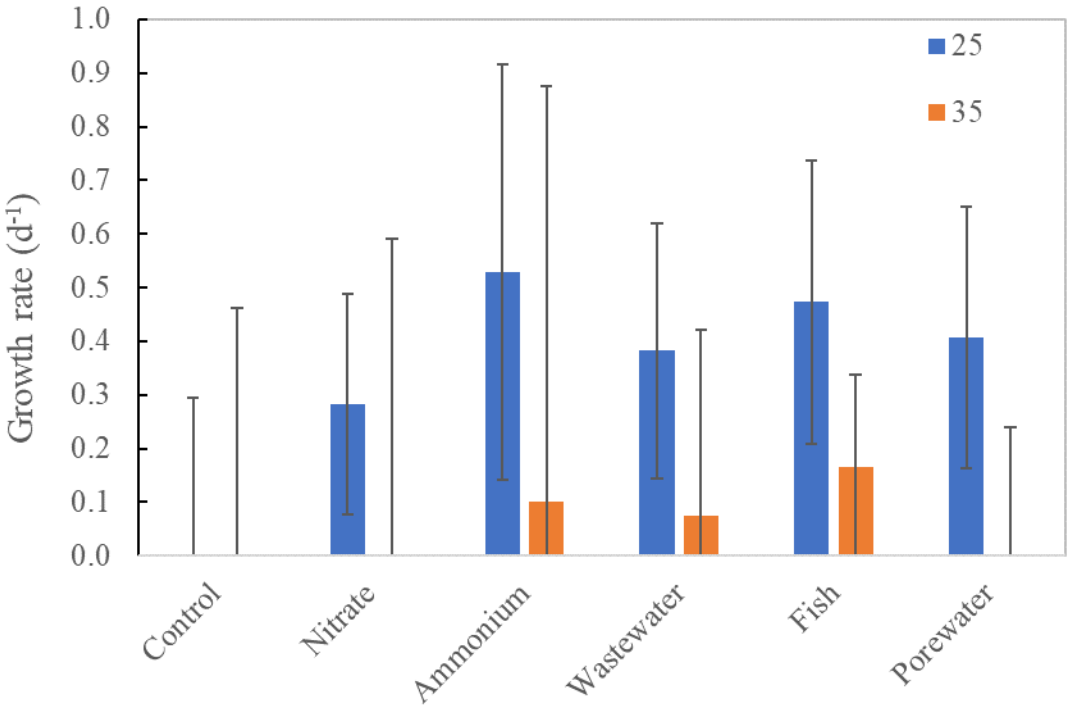

Figure 12. Growth rate of K. brevis at salinities of 25 (blue bars) and 35 (orange bars) in treatments with different nitrogen sources.

Discussion

In the natural environment, both nitrogen availability and salinity play an important role in modulating the growth of *K. brevis*. Results from these growth experiments likewise show a strong influence of salinity. Overall, highest growth rates were observed at a salinity of 25, while growth rates were much lower at salinity of 35. Lab and field studies have yielded varying

results on optimal salinity ranges, and there appears to be some degree of strain-specificity in the response to salinity. A literature review suggested that optimal growth salinities ranged from 25-45 (Vargo 2009), while others have found suboptimal growth outside of salinities between ~27 to 35-37 (e.g., Aldrich and Wilson 1960; Maier Brown et al 2006). Results from the accompanying field study (e.g., Figure 7) show a narrower range of optimal salinities in Corpus Christi Bay, ranging from the upper 20's to low 30's. More data is needed to verify this finding, but overall, results of both the field and lab experiments confirm an apparent influence of salinity on *K. brevis* growth. This is important in the context of historical changes that have occurred in Nueces and Corpus Christi Bays, specifically a long-term decrease in freshwater inflows which have presumably led to a transition from brackish conditions, at least in Nueces Bay, to more ocean-influenced conditions that would be optimal for *K. brevis*.

Given the range of variability in growth responses to nitrogen treatments, it is difficult to draw firm conclusions on nutrient preferences. In fact, results from the experiment conducted at a salinity of 25 showed that *K. brevis* was able to grow on any of the diverse array of nitrogen sources, including simple compounds of ammonium and nitrate as well as more complex sources from porewater, wastewater and dead fish. These findings are consistent with work conducted over the past decade on *K. brevis* in Florida, which showed that there is likely not one specific nutrient source supporting its growth and emphasizing the nutritional flexibility of the organism (e.g., Heil et al. 2014; Bronk et al. 2014). In the context of bloom dynamics and influences in local estuaries (to Nueces and Corpus Christi Bays), these findings indicate that it would be difficult to identify and manage specific nutrient sources to reduce bloom potential, especially when considering the multitude of possible internal and external sources to those bays.

References

Aldrich, D. v, and W. B. Wilson. 1960. The effect of salinity on growth of *Gymnodinium breve* Davis. *The Biological Bulletin* 119: 57–64.

Altman, J. C., and H. W. Paerl. 2012. Composition of inorganic and organic nutrient sources influences phytoplankton community structure in the New River Estuary, North Carolina. *Aquatic Ecology* 46: 269–282. https://doi.org/10.1007/s10452-012-9398-8.

Baden, D. G., and T. J. Mende. 1979. Amino acid utilization by Gymnodinium breve. *Phytochemistry* 18: 247–251. https://doi.org/10.1016/0031-9422(79)80063-1.

Baek, S. H., D. Kim, M. Son, S. M. Yun, and Y. O. Kim. 2015. Seasonal distribution of phytoplankton assemblages and nutrient-enriched bioassays as indicators of nutrient limitation of phytoplankton growth in Gwangyang Bay, Korea. *Estuarine, Coastal and Shelf Science* 163: 265–278. https://doi.org/10.1016/j.ecss.2014.12.035.

Barton, K. 2020. MuMIn: Multi-Model Inference.

Brand, L. E., L. Campbell, and E. Bresnan. 2012. Karenia: The biology and ecology of a toxic genus. Harmful Algae 14. Elsevier B.V.: 156–178. https://doi.org/10.1016/j.hal.2011.10.020.

Brand, L. E., and A. Compton. 2007. Long-term increase in *Karenia brevis* abundance along the Southwest Florida Coast. *Harmful Algae* 6: 232–252. https://doi.org/10.1016/j.hal.2006.08.005.

Breier, C. F., and E. J. Buskey. 2007. Effects of the red tide dinoflagellate, *Karenia brevis*, on grazing and fecundity in the copepod Acartia tonsa. *Journal of Plankton Research* 29: 115–126. https://doi.org/10.1093/plankt/fbl075.

Bricker, S. B., B. Longstaff, W. Dennison, A. Jones, K. Boicourt, C. Wicks, and J. Woerner. 2008. Effects of nutrient enrichment in the nation's estuaries: A decade of change. *Harmful Algae* 8: 21–32. https://doi.org/10.1016/j.hal.2008.08.028.

Bronk, D.A., L. Killberg-Thoreson, R.E. Sipler, M.R. Mulholland, Q.N. Roberts, P.W. Bernhard, M. Garrett, J.M. O'Neil, and C.A. Heil. 2014. Nitrogen uptake and regeneration (ammonium regeneration, nitrification and photoproduction) in waters of the West Florida Shelf prone to blooms of *Karenia brevis*. *Harmful Algae* 38: 50-62

Bugica, K., B. Sterba-Boatwright, and M. S. Wetz. 2020. Water quality trends in Texas estuaries. *Marine Pollution Bulletin* 152. https://doi.org/10.1016/j.marpolbul.2020.110903.

Buskey, E. J. 1996. Current Status and Historical Trends of Brown Tide and Red Tide Phytoplankton Blooms in the Corpus Christi Bay National Estuary Program Study Area Corpus Christi Bay National Estuary Program CCBNEP-07 •. Austin, Texas.

Chin, T. 2020. Comparison of phytoplankton biomass and community composition in three Texas estuaries differing in freshwater inflow regime. Thesis. Texas A&M University-Corpus Christi.

Cira, E. K., H. W. Paerl, and M. S. Wetz. 2016. Effects of nitrogen availability and form on phytoplankton growth in a eutrophied estuary (Neuse River Estuary, NC, USA). *PLoS ONE* 11: e0160663. https://doi.org/10.1371/journal.pone.0160663.

Cira, E. K., T. A. Palmer, and M. S. Wetz. 2021. Phytoplankton Dynamics in a Low-Inflow Estuary (Baffin Bay, TX) During Drought and High-Rainfall Conditions Associated with an El Niño Event. *Estuaries and Coasts* 1–13.

Clarke, K. R., and R. N. Gorley. 2015. Getting started with PRIMER v7. PRIMER-E: Plymouth, Plymouth Marine Laboratory: 20.

Cloern, J. E. 1999. The relative importance of light and nutrient limitation of phytoplankton growth: A simple index of coastal ecosystem sensitivity to nutrient enrichment. *Aquatic Ecology* 33: 3–19.

Cloern, J. E., and R. Dufford. 2005. Phytoplankton community ecology: Principles applied in San Francisco Bay. *Marine Ecology Progress Series* 285: 11–28. https://doi.org/10.3354/meps285011.

Cloern, J. E., and A. D. Jassby. 2008. Complex seasonal patterns of primary producers at the land-sea interface. *Ecology Letters* 11: 1294–1303. https://doi.org/10.1111/j.1461-0248.2008.01244.x.

Cloern, J. E., and A. D. Jassby. 2010. Patterns and scales of phytoplankton variability in estuarine-coastal ecosystems. *Estuaries and Coasts* 33: 230–241. https://doi.org/10.1007/s12237-009-9195-3.

Dardis, C. 2015. LogisticDx: Diagnostic Tests for Models with a Binomial Response.

Davis, C. C. 1948. Gymnodinium Brevis Sp. Nov., A Cause of Discolored Water and Animal Mortality in the Gulf of Mexico. *Botanical Gazette* 109: 358–360. https://doi.org/10.1086/335488.

Dixon, L. K., G. J. Kirkpatrick, E. R. Hall, and A. Nissanka. 2014. Nitrogen, phosphorus and silica on the West Florida Shelf: Patterns and relationships with Karenia spp. occurrence. *Harmful Algae* 38: 8–19. https://doi.org/10.1016/j.hal.2014.07.001.

Dorado, S., T. Booe, J. Steichen, A. S. McInnes, R. Windham, A. Shepard, A. E. B. Lucchese, et al. 2015. Towards an understanding of the interactions between freshwater inflows and phytoplankton communities in a subtropical estuary in the Gulf of Mexico. *PLoS ONE* 10. https://doi.org/10.1371/journal.pone.0130931.

Doucette, G. J., E. R. McGovern, and J. A. Babinchak. 1999. Algicidal bacteria active against Gymnodinium breve (Dinophyceae). I. Bacterial isolation and characterization of killing activity. *Journal of Phycology* 35: 1447–1454. https://doi.org/10.1046/j.1529-8817.1999.3561447.x.

Errera, R. M., S. Yvon-Lewis, J. D. Kessler, and L. Campbell. 2014. Reponses of the dinoflagellate *Karenia brevis* to climate change: PCO2 and sea surface temperatures. *Harmful Algae* 37: 110–116. https://doi.org/10.1016/j.hal.2014.05.012.

Ferreira, J. G., W. J. Wolff, T. C. Simas, and S. B. Bricker. 2005. Does biodiversity of estuarine phytoplankton depend on hydrology? *Ecological Modelling* 187: 513–523. https://doi.org/10.1016/j.ecolmodel.2005.03.013.

Fisher, T. R., A. B. Gustafson, K. Sellner, R. Lacouture, L. W. Haas, R. L. Wetzel, R. Magnien, D. Everitt, B. Michaels, and R. Karrh. 1999. Spatial and temporal variation of resource limitation in Chesapeake Bay. *Marine Biology* 133: 763–778. https://doi.org/10.1007/s002270050518.

Flaherty, K. E., and J. H. Landsberg. 2011. Effects of a Persistent Red Tide (*Karenia brevis*) Bloom on Community Structure and Species-Specific Relative Abundance of Nekton in a Gulf of Mexico Estuary. *Estuaries and Coasts* 34: 417–439. https://doi.org/10.1007/s12237-010-9350-x.

Geyer, N. L., M. Huettel, and M. S. Wetz. 2018. Phytoplankton Spatial Variability in the River-Dominated Estuary, Apalachicola Bay, Florida. *Estuaries and Coasts* 41: 2024–2038. https://doi.org/10.1007/s12237-018-0402-y.

Glibert, P. M., D. M. Anderson, P. Gentien, E. Granéli, and K. G. Sellner. 2005. The Global, Complex Phenomena of Harmful Algal Blooms. *Oceanography* 18: 136–147. https://doi.org/10.1016/B978-0-12-385876-4.00020-7.

Glibert, P. M., J. A. M. Burkholder, T. M. Kana, J. Alexander, H. Skelton, and C. Shilling. 2009. Grazing by *Karenia brevis* on *Synechococcus* enhances its growth rate and may help to sustain blooms. *Aquatic Microbial Ecology* 55: 17–30. https://doi.org/10.3354/ame01279.

Glibert, P. M., F. P. Wilkerson, R. C. Dugdale, J. A. Raven, C. L. Dupont, P. R. Leavitt, A. E. Parker, J. M. Burkholder, and T. M. Kana. 2016. Pluses and minuses of ammonium and nitrate uptake and assimilation by phytoplankton and implications for productivity and community composition, with emphasis on nitrogen-enriched conditions. *Limnology and Oceanography* 61: 165–197. https://doi.org/10.1002/LNO.10203@10.1002

Guinder, V. A., C. A. Popovich, J. C. Molinero, and G. M. E. Perillo. 2010. Long-term changes in phytoplankton phenology and community structure in the Bahía Blanca Estuary, Argentina. *Marine Biology* 157: 2703–2716. https://doi.org/10.1007/s00227-010-1530-5.

Harris, R. J., D. A. Arrington, D. Porter, and V. Lovko. 2020. Documenting the duration and chlorophyll pigments of an allochthonous *Karenia brevis* bloom in the Loxahatchee River Estuary (LRE), Florida. *Harmful Algae* 97: 101851. https://doi.org/10.1016/j.hal.2020.101851.

Hart, J. A., E. J. Phlips, S. Badylak, N. Dix, K. Petrinec, A. L. Mathews, W. Green, and A. Srifa. 2015. Phytoplankton biomass and composition in a well-flushed, sub-tropical estuary: The contrasting effects of hydrology, nutrient loads and allochthonous influences. *Marine Environmental Research* 112: 9–20. https://doi.org/10.1016/j.marenvres.2015.08.010.

Heil, C. A., L. K. Dixon, E. Hall, M. Garrett, J. M. Lenes, J. M. O'Neil, B. M. Walsh, et al. 2014. Blooms of *Karenia brevis* (Davis) G. Hansen & Ø. Moestrup on the West Florida Shelf: Nutrient sources and potential management strategies based on a multi-year regional study. *Harmful Algae* 38: 127–140. https://doi.org/10.1016/j.hal.2014.07.016.

Henrichs, D. W., R. D. Hetland, and L. Campbell. 2015. Identifying bloom origins of the toxic dinoflagellate *Karenia brevis* in the western Gulf of Mexico using a spatially explicit individual-based model. *Ecological Modelling* 313: 251–258. https://doi.org/10.1016/j.ecolmodel.2015.06.038.

Henrichs, D. W., M. C. Tomlinson, and L. Campbell. Predicting bloom initiation on the Texas (USA) coast: Combining satellite imagery with an individual-based model. HARMFUL ALGAE 2018–FROM ECOSYSTEMS TO SOCIO-ECOSYSTEMS: 55.

Hetland, R. D., and L. Campbell. 2007. Convergent blooms of *Karenia brevis* along the Texas coast. *Geophysical Research Letters* 34: 1–5. https://doi.org/10.1029/2007GL030474.

Holland, J., N. J. Maciolek, R. D. Kalke, L. Mullins, and C. H. Oppenheimer. A Benthos and Plankton Study of the Corpus Christi, Copano and Aransas Bay Systems III. Report on Data Collected During the Period July 1974-May 1975 and Summary of the Three-year Project.

Islam, M. S., J. S. Bonner, B. L. Edge, and C. A. Page. 2014. Hydrodynamic characterization of Corpus Christi Bay through modeling and observation. *Environmental Monitoring and Assessment* 186: 7863–7876. https://doi.org/10.1007/s10661-014-3973-5.

Jackman, S. 2020. pscl: Classes and Methods for R Developed in the Political Science Computational Laboratory. Sydney, New South Wales, Australia.

Jeong, H. J., J. Y. Park, J. H. Nho, M. O. Park, J. H. Ha, K. A. Seong, C. Jeng, C. N. Seong, K. Y. Lee, and W. H. Yih. 2005. Feeding by red-tide dinoflagellates on the cyanobacterium *Synechococcus*. *Aquatic Microbial Ecology* 41: 131–143.

Kubanek, J., T. W. Snell, and C. Pirkle. 2007. Chemical defense of the red tide dinoflagellate *Karenia brevis* against rotifer grazing. *Limnology and Oceanography* 52: 1026–1035. https://doi.org/10.4319/lo.2007.52.3.1026.

Landsberg, J. H., and K. A. Steidinger. 1988. A historical review of *Gymnodinium breve* red tides implicated in mass mortalities of the manatee (*Trichechus manatus latirostris*) in Florida, UAS. In Harmful Algae, 97–100. Xunta de Galicia and Intergovernmental Oceaographic Commission of UNESCO.

Lomas, M. W., and P. M. Glibert. 1999. Interactions between NH_4^+ and NO^{3-} uptake and assimilation: comparison of diatoms and dinoflagellates at several growth temperatures. *Marine Biology* 133: 541–551.

Magaña, H. A., C. Contreras, and T. A. Villareal. 2003. A historical assessment of *Karenia brevis* in the western Gulf of Mexico. *Harmful Algae* 2: 163–171. https://doi.org/10.1016/S1568-9883(03)00026-X.

Magaña, H. A., and T. A. Villareal. 2006. The effect of environmental factors on the growth rate of *Karenia brevis* (Davis) G. Hansen and Moestrup. *Harmful Algae* 5: 192–198. https://doi.org/10.1016/j.hal.2005.07.003.

Maier Brown, A. F., Q. Dortch, F. M. V. Dolah, T. A. Leighfield, W. Morrison, A. E. Thessen, K. Steidinger, B. Richardson, C. A. Moncreiff, and J. R. Pennock. 2006. Effect of salinity on the distribution, growth, and toxicity of *Karenia* spp. *Harmful Algae* 5: 199–212. https://doi.org/10.1016/j.hal.2005.07.004.

McHugh, K. A., J. B. Allen, A. A. Barleycorn, and R. S. Wells. 2011. Severe *Karenia brevis* red tides influence juvenile bottlenose dolphin (*Tursiops truncatus*) behavior in Sarasota Bay, Florida. *Marine Mammal Science* 27: 622–643. https://doi.org/10.1111/j.1748-7692.2010.00428.x.

Milroy, S. P., D. A. Dieterle, R. He, G. J. Kirkpatrick, K. M. Lester, K. A. Steidinger, G. A. Vargo, J. J. Walsh, and R. H. Weisberg. 2008. A three-dimensional biophysical model of *Karenia brevis* dynamics on the west Florida shelf: A look at physical transport and potential zooplankton grazing controls. *Continental Shelf Research* 28: 112–136. https://doi.org/10.1016/j.csr.2007.04.013.

Montagna, P. A., E. M. Hill, and B. Moulton. 2009. Role of science-based and adaptive management in allocating environmental flows to the Nueces Estuary, Texas, USA. *WIT Transactions on Ecology and the Environment* 122: 559–570. https://doi.org/10.2495/ECO090511.

Nielsen-Gammon, J., J. Banner, B. Cook, D. Tremaine, C. Wong, R. Mace, H. Gao, et al. 2020. Unprecedented drought challenges for Texas water resources in a changing climate: what do researchers and stakeholders need to know? Earth's Future 8. https://doi.org/10.1029/2020EF001552.

Nohe, A., A. Goffin, L. Tyberghein, R. Lagring, K. de Cauwer, W. Vyverman, and K. Sabbe. 2020. Marked changes in diatom and dinoflagellate biomass, composition and seasonality in the Belgian Part of the North Sea between the 1970s and 2000s. *Science of the Total Environment* 716. https://doi.org/10.1016/j.scitotenv.2019.136316.

Örnólfsdóttir, E. B., S. E. Lumsden, and J. L. Pinckney. 2004. Nutrient pulsing as a regulator of phytoplankton abundance and community composition in Galveston Bay, Texas. *Journal*

of Experimental Marine Biology and Ecology 303: 197–220. https://doi.org/10.1016/j.jembe.2003.11.016.

Pachauri, R. K., M. R. Allen, V. R. Barros, J. Broome, W. Cramer, R. Christ, J. A. Church, et al. 2014. Climate Change 2014: Synthesis Report. Contribution of Working Groups I, II and III to the Fifth Assessment Report of the Intergovernmental Panel on Climate Change. Edited by R K Pachauri and L Meyer. Geneva, Switzerland: IPCC.

Paerl, H. W., N. S. Hall, B. L. Peierls, and K. L. Rossignol. 2014. Evolving Paradigms and Challenges in Estuarine and Coastal Eutrophication Dynamics in a Culturally and Climatically Stressed World. *Estuaries and Coasts* 37. https://doi.org/10.1007/s12237-014-9773-x.

Paerl, H. W., and D. Justic. 2013. Estuarine phytoplankton. In Estuarine ecology, Second, 85–110. Wiley Online Library.

Paul, J. H., L. Houchin, D. Griffin, T. Slifko, M. Guo, B. Richardson, and K. Steidinger. 2002. A filterable lytic agent obtained from a red tide bloom that caused lysis of *Karenia brevis* (Gymnodinum breve) cultures. *Aquatic Microbial Ecology* 27: 21–27. https://doi.org/10.3354/ame027021.

Pinckney, J. L., H. W. Paerl, M. B. Harrington, and K. E. Howe. 1998. Annual cycles of phytoplankton community-structure and bloom dynamics in the Neuse River Estuary, North Carolina. *Marine Biology* 131: 371–381. https://doi.org/10.1007/s002270050330.

Pinckney, James L, H. W. Paerl, P. Tester, and T. L. Richardson. 2001. The role of nutrient loading and eutrophication in estuarine ecology. *Environmental health perspectives* 109: 699–706.

Poulson-Ellestad, K. L., C. M. Jones, J. Roy, M. R. Viant, F. M. Fernández, J. Kubanek, and B. L. Nunn. 2014. Metabolomics and proteomics reveal impacts of chemically mediated competition on marine plankton. *Proceedings of the National Academy of Sciences* 111: 9009–9014. https://doi.org/10.1073/pnas.1402130111.

Prince, E. K., T. L. Myers, and J. Kubanek. 2008. Effects of harmful algal blooms on competitors: Allelopathic mechanisms of the red tide dinoflagellate *Karenia brevis*. *Limnology and Oceanography* 53: 531–541. https://doi.org/10.4319/lo.2008.53.2.0531.

Prince, E. K., K. L. Poulson, T. L. Myers, R. D. Sieg, and J. Kubanek. 2010. Characterization of allelopathic compounds from the red tide dinoflagellate *Karenia brevis*. *Harmful Algae* 10: 39–48. https://doi.org/10.1016/j.hal.2010.06.003.

R Core Team. 2019. R: A Language and Environment for Statistical Computing. Vienna, Austria.

Reyna, N. E., A. K. Hardison, and Z. Liu. 2017. Influence of major storm events on the quantity and composition of particulate organic matter and the phytoplankton community in a subtropical estuary, Texas. *Frontiers in Marine Science* 4: 43.

Ritter, C., and P. A. Montagna. 1999. Seasonal hypoxia and models of benthic response in a Texas Bay. *Estuaries* 22: 7–20. https://doi.org/10.2307/1352922.

Roelke, D. L., L. A. Cifuentes, and P. M. Eldridge. 1997. Nutrient and phytoplankton dynamics in a sewage-impacted gulf coast estuary: A field test of the PEG-model and Equilibrium Resource Competition theory. *Estuaries* 20: 725–742. https://doi.org/10.2307/1352247.

Roelke, D. L., P. M. Eldridge, and L. A. Cifuentes. 1999. A model of phytoplankton competition for limiting and nonlimiting nutrients: Implications for development of estuarine and nearshore management schemes. *Estuaries* 22: 92–104. https://doi.org/10.2307/1352930.

Roelke, Daniel L., H. P. Li, N. J. Hayden, C. J. Miller, S. E. Davis, A. Quigg, and Y. Buyukates. 2013. Co-occurring and opposing freshwater inflow effects on phytoplankton biomass, productivity and community composition of Galveston Bay, USA. *Marine Ecology Progress Series* 477: 61–76. https://doi.org/10.3354/meps10182.

Roth, P. B., M. J. Twiner, C. M. Mikulski, A. B. Barnhorst, and G. J. Doucette. 2008. Comparative analysis of two algicidal bacteria active against the red tide dinoflagellate *Karenia brevis*. *Harmful Algae* 7: 682–691. https://doi.org/10.1016/j.hal.2008.02.002.

Shangguan, Y., P. M. Glibert, J. A. Alexander, C. J. Madden, and S. Murasko. 2017. Nutrients and phytoplankton in semienclosed lagoon systems in Florida Bay and their responses to changes in flow from Everglades restoration. *Limnology and Oceanography* 62: S327–S347. https://doi.org/10.1002/lno.10599.

Sinclair GA and D Kamykowski (2006) Benthic-pelagic coupling in sediment-associated populations of *Karenia brevis*. Journal of Plankton Research 30(7):829-838.

Smith, T. J., and C. M. McKenna. 2013. A Comparison of Logistic Regression pseudo R2 indices. *Multiple Linear Regression Viewpoints* 39: 17–26.

de Souza, K. B., T. Jephson, T. B. Hasper, and P. Carlsson. 2014. Species-specific dinoflagellate vertical distribution in temperature-stratified waters. *Marine Biology* 161: 1725–1734. https://doi.org/10.1007/s00227-014-2446-2.

Steidinger, K. A. 2009. Historical perspective on *Karenia brevis* red tide research in the Gulf of Mexico. *Harmful Algae* 8: 549–561. https://doi.org/10.1016/j.hal.2008.11.009.

Steidinger, K. A., and R. M. Ingle. 1972. Observations on the 1971 summer red tide in Tampa Bay, Florida. *Environmental Letters* 3: 271–278.

Stumpf, R. P., R. W. Litaker, L. Lanerolle, and P. A. Tester. 2008. Hydrodynamic accumulation of *Karenia* off the west coast of Florida. *Continental Shelf Research* 28: 189–213. https://doi.org/10.1016/j.csr.2007.04.017.

Suggett, D. J., C. M. Moore, A. E. Hickman, and R. J. Geider. 2009. Interpretation of fast repetition rate (FRR) fluorescence: Signatures of phytoplankton community structure versus physiological state. *Marine Ecology Progress Series* 376: 1–19. https://doi.org/10.3354/meps07830.

Sun, J., and D. Liu. 2003. Geometric models for calculating cell biovolume and surface area for phytoplankton. *Journal of Plankton Research* 25: 1331–1346. https://doi.org/10.1093/plankt/fbg096.

Sverdrup, H. U. 1953. On conditions for the vernal blooming of phytoplankton. *ICES Journal of Marine Science* 18: 287–295.

Tester, P. A., and K. A. Steidinger. 1997. *Gymnodinium breve* red tide blooms: Initiation, transport, and consequences of surface circulation. *Limnology and Oceanography* 42. Wiley-Blackwell: 1039–1051. https://doi.org/10.4319/lo.1997.42.5_part_2.1039.

Thyng, K. M., R. D. Hetland, M. T. Ogle, X. Zhang, F. Chen, and L. Campbell. 2013. Origins of *Karenia brevis* harmful algal blooms along the Texas coast . *Limnology and Oceanography: Fluids and Environments* 3: 269–278. https://doi.org/10.1215/21573689-2417719.

Tolan, J. M. 2007. El Niño-Southern Oscillation impacts translated to the watershed scale: Estuarine salinity patterns along the Texas Gulf Coast, 1982 to 2004. *Estuarine, Coastal and Shelf Science* 72: 247–260. https://doi.org/10.1016/j.ecss.2006.10.018.

Tominack, S. A., K. Z. Coffey, D. Yoskowitz, G. Sutton, and M. S. Wetz. 2020. An assessment of trends in the frequency and duration of *Karenia brevis* red tide blooms on the South Texas coast (western Gulf of Mexico). Edited by Just Cebrian. *PLOS ONE* 15: e0239309. https://doi.org/10.1371/journal.pone.0239309.

Tominack, S. A. 2021. Phytoplankton dynamics in an urbanizing South Texas estuary, Corpus Christi Bay, Texas. Dissertation. Texas A&M University-Corpus Christi.

Turner, E. L., B. Paudel, and P. A. Montagna. 2015. Baseline nutrient dynamics in shallow well mixed coastal lagoon with seasonal harmful algal blooms and hypoxia formation. *Marine Pollution Bulletin* 96: 456–462. https://doi.org/10.1016/j.marpolbul.2015.05.005.

Vargo, G. A. 2009. A brief summary of the physiology and ecology of *Karenia brevis* Davis (G. Hansen and Moestrup comb. nov.) red tides on the West Florida Shelf and of hypotheses posed for their initiation, growth, maintenance, and termination. *Harmful Algae* 8: 573–584. https://doi.org/10.1016/j.hal.2008.11.002.

Vargo, G. A., C. A. Heil, K. A. Fanning, L. K. Dixon, M. B. Neely, K. Lester, D. Ault, et al. 2008. Nutrient availability in support of *Karenia brevis* blooms on the central West Florida Shelf: What keeps Karenia blooming? Shelf Research 28: 73–98. https://doi.org/10.1016/j.csr.2007.04.008.

Waggett, R. J., D. R. Hardison, and P. A. Tester. 2012. Toxicity and nutritional inadequacy of *Karenia brevis*: Synergistic mechanisms disrupt top-down grazer control. Ecology Progress Series 444: 15–30. https://doi.org/10.3354/meps09401.

Walker, D. A., and T. J. Smith. 2016. JMASM algorithms and code nine pseudo R2 indices for binary logistic regression models. *Journal of Modern Applied Statistical Methods* 15: 848–854. https://doi.org/10.22237/jmasm/1462077720.

Walsh, B. M., and J. M. O'Neil. 2014. Zooplankton community composition and copepod grazing on the West Florida Shelf in relation to blooms of *Karenia brevis*. *Harmful Algae* 38: 63–72. https://doi.org/10.1016/j.hal.2014.04.011.

Walsh, J.J., and 24 others. 2006. Red tides in the Gulf of Mexico: Where, when, and why? J. Geophysical Research-Oceans 111: doi:10.1029/2004JC002813

Walsh, J. J., R. H. Weisberg, J. M. Lenes, F. R. Chen, D. A. Dieterle, L. Zheng, K. L. Carder, et al. 2009. Isotopic evidence for dead fish maintenance of Florida red tides, with implications for coastal fisheries over both source regions of the West Florida shelf and within downstream waters of the South Atlantic Bight. *Progress in Oceanography* 80: 51–73. https://doi.org/10.1016/j.pocean.2008.12.005.

Walters, S., S. Lowerre-Barbieri, J. Bickford, J. Tustison, and J. H. Landsberg. 2013. Effects of *Karenia brevis* red tide on the spatial distribution of spawning aggregations of sand seatrout *Cynoscion arenarius* in Tampa Bay, Florida. *Marine Ecology Progress Series* 479: 191–202. https://doi.org/10.3354/meps10219.

Winder, M., and U. Sommer. 2012. Phytoplankton response to a changing climate. *Hydrobiologia* 698: 5–16. https://doi.org/10.1007/s10750-012-1149-2.

Task 3: Outreach Efforts

Education and outreach were vital components of this study. One Ph.D. student (Sarah Tominack) built her dissertation using data from this project, while three M.S. students (Tiffany Chin, Jordana Cutajar, Molly McBride) and three undergraduates (Felipe Urrutia, Vanessa Navarro, Isabelle Cummings) received training in methods used and assisted with data collection for the study. Results from this study were presented in several venues including classroom presentations, public seminars, and scientific conferences. Below is a list of outreach and education efforts that were undertaken as part of this study. Ongoing or future planned efforts will be reported to GLO as they occur. Supporting documents will be provided to GLO separately.

Presentations (scientific conferences):

- Cutajar, J., and M. Wetz. 2021. Spatial-temporal variability in phytoplankton biomass and community composition in Texas residential canals. Coastal & Estuarine Research Federation Meeting.

Presentations (public, local):

- Wetz, M. 2021. Human and climate-driven water quality challenges affecting the Texas coast. Clean Coast Texas, October Lunch-and-Learn series.
- Wetz, M. 2021. Human and climate-driven water quality challenges affecting the Texas coast. Friday Morning Club, Corpus Christi, Texas.

Presentations (university class):

- Wetz, M. 4/20/2021 lecture. Harmful algal blooms. BIOL 4328 (Global Change Ecology), Texas A&M University-Corpus Christi, 20 undergraduates enrolled.